FIELD APPLICATIONS OF THE FAST MARCHING METHOD ON SHALE GAS RESERVOIRS

A Thesis

by

NEHA BANSAL

Submitted to the Office of Graduate and Professional Studies of
Texas A&M University
in partial fulfillment of the requirements for the degree of

MASTER OF SCIENCE

Chair of Committee,	Akhil Datta-Gupta
Committee Members,	Michael J. King
	Yuefeng Sun
Head of Department,	Dan Hill

May 2014

Major Subject: Petroleum Engineering

ABSTRACT

Unconventional resources derive their name based on the unconventional evaluation, extraction and production requirements associated with them. Unconventional reservoirs have moved from emerging resources a decade ago to major interests of many operating companies. The remarkable increase in the stakes of these reservoirs and the growth of associated risk has pushed the industry to update and upgrade evaluation techniques of such reservoirs. Current industry practice for characterization and assessment of unconventional reservoirs mostly utilizes empirical decline curve analysis or analytic rate and pressure transient analysis.

Analytical techniques are not capable to include the flow dynamics of a full field numerical simulation model for its capabilities to capture field geology, reservoir geometry and property distribution. Whereas, a reservoir simulation model requires detailed information input set and is computationally expensive. Fast marching method has been introduced as an intermediate approach to overcome the limitations of analytical techniques and as a complimentary tool to numerical simulation. This approach is based on a high frequency asymptotic solution of the diffusivity equation in heterogeneous reservoirs. This leads to Eikonal equation which can be solved for 'diffusive time of flight', governing pressure front propagation in the reservoir. The Eikonal equation is solved using fast marching method giving the speed to the solution. Diffusive time of flight can be a useful tool for drainage volume visualization and well

performance prediction. It can further be used as spatial coordinates to reduce 3-D diffusivity equation into a 1-D equation thereby making it a comprehensive simulator. The speed and versatility of our proposed method makes it ideally suited for high resolution reservoir characterization through integration of static and dynamic data.

The major advantages of the approach are its simplicity, intuitive appeal and computational efficiency. This work demonstrates power and utility of our method using a field example that involves history matching, uncertainty analysis and performance assessment of a shale gas reservoir located in East Texas. A sensitivity study is first carried out to systematically identify the 'heavy hitters' impacting the well performance. This is followed by a history matching and uncertainty analysis to identify the fracture parameters and the stimulated reservoir volume. A comparison of model predictions with the actual well performance shows that our approach is able to reliably predict the pressure depletion and rate decline.

DEDICATION

To my grandmother, parents and sister

For their endless support, love and encouragement

ACKNOWLEDGEMENTS

I would like to thank my committee chair, Dr. Akhil Datta-Gupta, who has been a tremendous support and guide. Sincere thanks to my other committee members, Dr. Michael King, and Dr. Yuefeng Sun, for their guidance during the course of this research.

A special thanks to all the members of MCERI research group for sharing their knowledge and lending me their support. Every person that I met during the course of my masters has had an influence on my work. I wish to be able to apply all the positive things I tried to learn from everyone during this time.

This work would not have been possible without the support from Anadarko Petroleum Corporation. I would like to thank the reservoir technology team for providing the material for the case study along with the constant feedback and help.

In the end, this journey would not feel the same without the support of my loving family and friends. Their words of encouragement were always my best guides even the moments of darkness.

NOMENCLATURE

k	Permeability, md
r	Radius of investigation, ft
t	Time, hours
c_t	Total compressibility, $psia^{-1}$
D	Standard finite difference operator
b	Decline rate
h	Formation thickness, ft
ρ	Gas density, lbm/cu ft
p	Pressure, psia
Z	Compressibility factor, fraction
$w(\tau)$	Derivative of the drainage pore volume w.r.t the diffusive time of flight
$\tilde{\mu}$	Dimensionless viscosity
$\tilde{c}_t$	Dimensionless total compressibility
Γ	Transfer function between matrix and fracture
σ	Geometric shape factor
$v(\tau)$	Derivative of the bulk volume with respect to τ
M	Property multiplier
S_{wi}	Irreducible water saturation, fraction

Subscripts

up	Upstream
f	Fracture
i	Initial
m	Matrix

Greek variables

α	Hydraulic diffusivity
τ	Diffusive time of flight
μ	Fluid viscosity
ϕ	Porosity
β	Geometric factor

Abbreviations

FMM	Fast Marching Method
SRV	Stimulated Reservoir Volume
SEPD	Stretched Exponential Production Decline
PDA	Production Data Analysis
RPI	Reciprocal Productivity Index
PLE	Power Law Exponential
SE	Stretched Exponential
DTOF	Diffusive Time of Flight

MCERI	Model Calibration and Efficient Reservoir Imaging
FDSIM	Finite Difference Simulator
BHP	Bottom hole pressure
GA	Genetic Algorithm

TABLE OF CONTENTS

Page

LIST OF FIGURES

Page

LIST OF TABLES

Page

CHAPTER I

LITERATURE REVIEW AND INTRODUCTION

Rise in demand, boom in prices, technical and engineering advances have made unconventional resources a significant part of the industry over the years. Especially, shale gas has been gathering a lot of attention for its potential as well as uncertainties surrounding its commercial viability and our understanding of its fundamental mechanisms itself. Further work is going on to improve modeling and forecasting of static and dynamic data to boost confidence for unconventional reservoir development.

To address production data, a number of methods have been introduced in the literature for example decline curve analysis (Arps, 1945; Fetkovich, 1980; Valko, 2009), diagnostic methods (Crafton, 1997;Palacio et al, 1993; Araya et al, 2002; Kabir et al, 2011) and many others. Fast marching method has been introduced in literature as a beneficial and extremely fast method to evaluate and visualize a number of parameters like drainage volume, pressure and rate solutions etc. before moving on to a more expensive, detailed and much more time consuming approach of reservoir simulation.

All the methods have their respective advantages and shortcomings. These methods need to be applied according to requirement of a particular study. A summary of evolution of various methods over the years along with a discussion on their applicability will be presented.

This chapter reviews the existing techniques available to analyze production data. The following chapter will review fast marching method for applications on unconventional reservoirs.

1. 1 Literature Review

During appraisal stage, determination of a well's most probable future and estimation of future production with data insufficiency for volumetric calculations, are some of challenges faced (Arps 1945) by the engineer. Decline curve analysis matches the production decline with a trend function and reserve estimation is done by extrapolation to an abandonment rate. The equations presented by Arps, act as fundamentals for most of the decline curve analysis techniques available today.

Fetkovitch (1980) recognized that results obtained from rate-time decline curve analysis can have multiple interpretations depending on the user. As an extension to Slider (1968) overlay method for analysis of rate-time data, a type curve approach was introduced to provide a more unique and "unbiased" solution. He introduced log-log type curve to handle transient as well as finite reservoir systems. These type curves could handle all the type of declines proposed by Arps (1945).

However, decline curve analysis method works on the assumption that a mathematical relation in past production will determine the future behavior, making the method strictly empirical. Further, the analysis is based on assumption of a constant bottom hole

pressure condition, which might not hold true all the time. Ilk et al. 2010; Ilk et al. 2008 also show that Arps method can provide optimistic results for unconventional reservoirs.

Problems of application of traditional decline curve analysis techniques directly on unconventional reservoirs have been reported often in the literature. Valko (2009) introduced a new decline curve analysis technique, developed specifically for shale gas reservoirs. Unlike traditional decline curve methods, rapid production changes could be detected and accounted for. Field applicability of the new method was shown extensively, using Barnett Shale well data.

An extension of this work (Valko and Lee 2010) was introduced for additional general applicability on unconventional wells in form of stretched exponential production decline (SEPD). The extension was helpful to improve on issues faced by industry, like applicability of hyperbolic decline model for tight reservoirs due to unsure boundary dominated state or traditional decline curve models on unconventional reservoirs. Authors noted two most significant advantages for this method include; finite value of estimated ultimate recovery (a condition violated in hyperbolic decline for $b \geq 1$) and recovery potential's linear relation with cumulative production. Another important contribution is the amalgamation of SEPD model and data-intensive discovery.

Can and Kabir (2011) proposed a workflow for reserve estimation of unconventional reservoirs based on SEPD. The workflow has applications on well with production

history and new wells without production data. Proposed workflow derives motivation from the need to apply probabilistic decline curve analysis on unconventional reservoirs owing to field maturity considerations, complexity in completions and fluid flow behavior. Method investigates coupling of probabilistic forecasting with decline curve analysis including SEPD. The method shows promising results even to handle large datasets in comparison to per well basis approach suggested in literature before. Literature supports the application advantages of SEPD over Arps' hyperbolic relation in the case of unconventional reservoirs.

Ilk et al. (2010) gave insight into challenges related to production data analysis. The work set out some guidelines helpful for analysis of production data along with challenges and mistakes that could be made. Authors also noted the scarcity in literature on diagnostic methods for production-data analysis in comparison to pressure transient analysis. This has been attributed to better quality and high frequency/high resolution nature of pressure-transient data in comparison to production data which in many cases is roughly estimated.

Authors proposed a simple workflow for a generic production data analysis for the user to understand the characteristics of the data before attempting to analyze it. A summary of basic checklist that a user could perform on time, pressure and rate data was also provided along with possible issues faced by user and common reasons behind lack in data correlations. This work emphasized on the importance of diagnostic plots for

production data analysis (PDA) and categorized these plots in three main categories. The first type deals with history and data correlation. The second type is used for reservoir diagnostics using log-log plots for identifying type of reservoir model. Final category is auxiliary diagnostic plots for reserve estimation.

Ilk et al. (2012) provided a workflow to analyze production data for unconventional "liquid-rich" reservoirs sighting Eagle Ford Shale a field study. Authors listed flow regime identification, completion efficiency, well performance evaluation and grouping, along with EUR trend establishment as the key objectives for PDA. The study demonstrated the application on nine wells. Following the previous works, the study suggested the importance of diagnostic interpretation before moving on to model based PDA and numerical simulation study. Difference in EUR trends or time function plots has been attributed to difference in well completions. The work suggests the use of nonlinear simulation study, to consider multiphase flow and other nonlinear effects. Also, the use of appropriate flow model has been found very crucial in forecasting study.

Medeiros et al. (2010) suggested drainage area estimation is an important and a primary goal for production analysis especially for tight formations like shale, as they produce primarily from stimulated reservoir volume.

Crafton (1997) proposed a reciprocal productivity index (RPI) method i.e. pressure normalized by rate to incorporate rate and pressure time-dependence. Author noted that

type curve analysis might fetch incorrect results in some cases as cross validation procedures have not been very applicable to these methods. Also history matching procedures are known to be highly sensitive to noise in the data and results are dependent on user's selection of model and tool. Method introduced by Crafton had an edge over traditional decline curve analysis with capability to determine reservoir properties like effective permeability-thickness (kh), skin and drainage area. It was presented as a combination of transient and decline analysis.

Palacio and Blasingame (1993) used rate normalization of pressure to propose a type curve matching for decline curve analysis. This study also introduced material balance time function used to derive pseudo steady state gas equation in the same form as liquid case.

Araya and Ozkan (2002) introduced dimensionless transient productivity index. Since the parameter's dependence on bottom hole conditions was negligible; same set of type curves could be used for different bottom hole rate and pressure conditions. Same can be extended to a gas case using pseudopressure and pseudotime.

Kabir et al. (2011) demonstrated the use of various analytical and numerical methods available for application on tight oil wells. Authors used a synthetic case and four field case studies to demonstrate the long-term production forecast capability of various decline curve methods; Arps, Power law exponential (PLE) and Stretched exponential

(SE). Their study suggested two most common flow regimes in such reservoirs; linear flow regime and transitional period. Testing of solutions was done using curve fitting for two separate time sections to forecast for 40years. The results show the consistency in SE solutions unlike arps and PLE, even when considered for different time segments. Authors presented that decline curve analysis tools work well for tight oil reservoirs for bounded region estimation. The SE gave more cautious but consistent projection and Aprs approach gave a slightly liberal estimation.

Mattar et al. (2008) presented various production evaluation techniques for shale gas systems, with emphasis on well geometry and stimulation. Authors noted that, estimation of reservoir properties and production forecasting are two main components in shale gas reservoir evaluation. While discussing production data analysis techniques in detail, authors discuss the production responses of common fracture systems like bi-wing, distributed and hybrid wing/SRV fracture systems. This was followed by analytical approach using type curves for vertical wells on field and simulated cases. The empirical approach was demonstrated by use of power-law exponential decline curve analysis proposed by Ilk et al. (2008). The technique was also tested for multiple transverse fracture horizontal wells. Study suggested that shale gas system forecasting could be done with some confidence using PLE method including forecasting for horizontal wells with multiple fractures. As suggested by many authors, use of hyperbolic decline for shale wells needs caution due to lack of boundary dominated flow in field history owing to extremely low permeability encountered.

1.2 Introduction

The objective of this work is to summarize and analyze the current techniques available for evaluation of unconventional reservoirs. One of the main objectives of this work is to present the first field case study of a shale gas reservoir with application of fast marching method. The advantages and capabilities of the emerging technique of fast marching method will also be presented.

Chapter II will give a background and summary of evolution of fast marching method in petroleum industry over the years. A synthetic case study will also be presented to show the capability of the fast marching method when compared to standard techniques like analytical or numerical simulation methods.

Chapter III provides details of the data provided by the Anadarko Petroleum Corporation (APC) for case study. A conventional production data analysis has also been conducted on the production data provided and this will also be presented as a section in this chapter.

In Chapter IV, we present two case studies; Case I and Case II respectively. Chapter includes details of model description, sensitivity study and history matching done on the field case study.

Chapter V includes the workflow used to test applicability of the fast marching method on a field study.

The final chapter (Chapter VI) will present discussion on results, conclusion and scope for future work.

CHAPTER II

FAST MARCHING METHOD*

This chapter summarizes the evolution of fast marching method (FMM) and discusses the applicability to field case.

2.1 Background

Depth of investigation is an important parameter especially with respect to unconventional reservoirs due to their extremely low permeability values. This attributes to production in unconventional reservoirs being mainly drawn from transient flow regime only. **Eq. (1)** is used for radius of investigation, in field units (Lee et al. 2003).

$$r = \sqrt{\frac{kt}{948\phi\mu c_t}} \qquad (1)$$

where,

r, radius of investigation (ft);

k, permeability (md);

t, time (hours);

ϕ, porosity (fraction);

*Certain sections reprinted with permission from "From Streamlines to Fast Marching: Rapid Simulation and Performance Assessment of Shale Gas Reservoirs Using Diffusive Time of Flight as a Spatial Coordinate" by Zhang, Y., Bansal, N., Fujita, Y., Datta-Gupta, A., King, M.J., Sankaran, S., 2014. Paper SPE 168997 presented at SPE Unconventional Resources Conference – USA, The Woodlands, Texas, USA, 1-3 April. Copyright 2014 by SPE.

c_t, total compressibility ($psia^{-1}$);

Generalized form of the above equation (Zhang et al. 2013) can be seen in **Eq. (2)** and **Eq. (3)**:

$$r = \sqrt{\beta \alpha t} \qquad (2)$$

$$\alpha = \frac{k}{\emptyset \mu c_t} \qquad (3)$$

where,

β, geometric factor for different flow patterns (2,4 and 6) (Kim et al. 2009);

α, hydraulic diffusivity;

For heterogeneous reservoirs, concept of diffusive time of flight was introduced by Vasco et al. (2000) and Kulkarni et al. (2000) using Eikonal equation for pressure front propagation. Xie et al. (2012) derived a solution to diffusive pressure equation by revisiting asymptotic solution emphasizing on Eikonal equation. **Eq. (4)** represents, pressure front propagation in an isotropic medium. The pressure front velocity of propagation in reservoir equals square root of diffusivity.

$$\sqrt{\alpha}\ |\nabla \tau(x)| = 1 \qquad (4)$$

where,

$\tau(x)$, diffusive time of flight;

Diffusive time of flight along a ray path can be calculated from **Eq. (5).**

$$\tau(r) = \int_0^r \frac{1}{\sqrt{\alpha}}\, dr' \quad \ldots\ldots\ldots\ldots\ldots\ldots\ldots\ldots\ldots\ldots\ldots\ldots\ldots\ldots\ldots (5)$$

where,

r, distance from well;

Eikonal equation can be solved efficiently using Fast marching methods (Sethian, 1999). The speed for the solution is due to the single pass nature of the method which is illustrated using 5-stencil Cartesian grid in Figure 1:

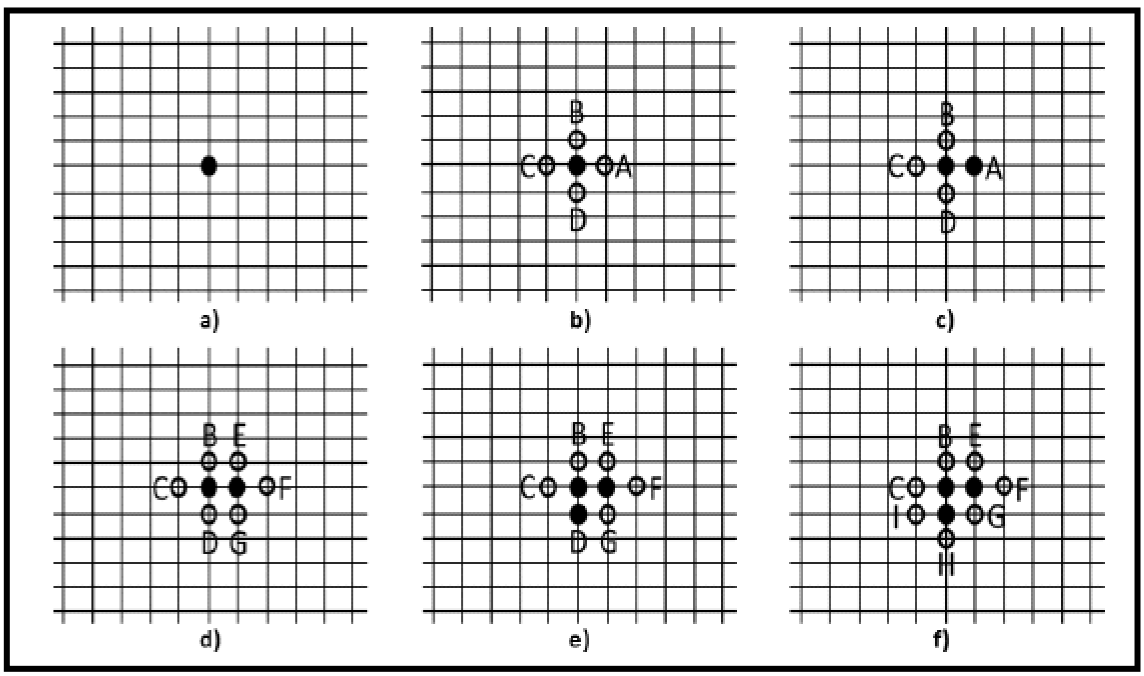

Figure 1: FMM illustration (Xie et. al 2012)

Following are the steps used for calculation from top left to right:

1. Label well location(producer/injector) as an accepted point with τ = 0

2. Mark all neighboring points A,B,C,D and calculate diffusive time of flight all neighboring points
3. Pick the minimum local solution for neighboring points and label it as accepted point in current neighboring points
4. Include the new neighboring points for accepted point for consideration
5. Repeat step 3 and 4 till all points in grid are accepted.

Sethian (1996) approach is used to calculate τ by discretizing Eikonal equation on 2-D rectangular grids as shown in **Eq. (6)**:

$$\max\left(D_{ij}^{-x}\,\tau, -D_{ij}^{+x}\,\tau, 0\right)^2 + \max\left(D_{ij}^{-y}\,\tau, -D_{ij}^{+y}\,\tau, 0\right)^2 = \frac{1}{\alpha} \quad \ldots\ldots\ldots\ldots\ldots\ldots\ldots\ldots\ldots\ldots (6)$$

where,

D, standard finite difference operator;

Eq. (7) and **Eq. (8)**: are expansions of D in ±x directions.

$$D_{ij}^{-x}\,\tau = \frac{(\tau_{i,j} - \tau_{i-1,j})}{\Delta x} \quad \ldots\ldots\ldots\ldots\ldots\ldots\ldots\ldots\ldots\ldots\ldots\ldots\ldots\ldots\ldots\ldots\ldots\ldots\ldots\ldots (7)$$

$$D_{ij}^{+x}\,\tau = \frac{(\tau_{i+1,j} - \tau_{i,j})}{\Delta x} \quad \ldots\ldots\ldots\ldots\ldots\ldots\ldots\ldots\ldots\ldots\ldots\ldots\ldots\ldots\ldots\ldots\ldots\ldots\ldots\ldots (8)$$

Eq. (9) and **Eq. (10)** are expansions of D in ±y directions.

$$D_{ij}^{-y}\,\tau = \frac{(\tau_{i,j} - \tau_{i,j-1})}{\Delta y} \quad \ldots\ldots\ldots\ldots\ldots\ldots\ldots\ldots\ldots\ldots\ldots\ldots\ldots\ldots\ldots\ldots\ldots\ldots\ldots\ldots (9)$$

$$D_{ij}^{+y}\,\tau = \frac{(\tau_{i,j+1} - \tau_{i,j})}{\Delta y} \quad \ldots\ldots\ldots\ldots\ldots\ldots\ldots\ldots\ldots\ldots\ldots\ldots\ldots\ldots\ldots\ldots\ldots\ldots\ldots\ldots (10)$$

Fast marching method (FMM) for unconventional reservoirs (Datta-Gupta et al. 2011, Xie et al. 2012a, 2012b; Zhang et al. 2013) has been proposed as a midway approach between analytical and numerical models. Xie et al. (2012) proposed FMM as a novel approach to compute and visualize depth of investigation along with geometric pressure solution to estimate transient pressure behavior. Zhang et al. (2013) extended the approach to corner point grids and anisotropic properties to extend the applications of the method.

FMM is based on the definition of depth of investigation (Lee 1982) as propagation distance of 'peak' pressure disturbance. Xie et al. (2012) used asymptotic solution of the diffusivity equation to derive an equation of pressure 'front' in the form of Eikonal equation. A solution of the same was introduced using fast marching methods (Sethian 1999). A successful generalization of depth of investigation of heterogeneous reservoirs to calculate drainage volume and a physical time map was also introduced.

Zhang et al. (2014) introduced the concept of using diffusive time of flight as spatial coordinates to rewrite diffusivity equation. This essentially helped to reduce a 3D problem into 1D problem to calculate pressure and rate solutions using diffusive time of flight. This new formulation has been used for simulating the performance of unconventional reservoirs in this work.

2.2 1-D Pressure/Rate Calculation Using Diffusive Time of Flight

Mass conservation equation is based on Darcy's law and has flux and accumulation terms as given by **Eq. (12)**.

$$\nabla \cdot \left(\frac{\rho}{\mu} k \nabla p\right) = \frac{\partial(\rho\phi)}{\partial t} \quad (12)$$

where,

ρ, gas density;

p, pressure;

We get **Eq. (13)** after applying chain rule on right hand side, substituting ρ using equation of state of gas based on real gas law, rearranging and replacing for rock and gas compressibility for total compressibility.

$$\nabla \cdot \left(\frac{p}{\mu Z} k \nabla p\right) = \phi \frac{p}{Z} c_t \frac{\partial p}{\partial t} \quad (13)$$

Eq. (13) can be transformed in 1-D coordinates to **Eq. (14)**, **Eq. (15)** and **Eq. (16)** using **Eq. (3)** and **Eq. (4).** Here, diffusive time of flight is calculated based on trajectory of pressure propagation from well as explained in previous section using the FMM.

$$\frac{\partial}{\partial \tau}\left(w(\tau) \frac{p}{\tilde{\mu} Z} \frac{\partial p}{\partial \tau}\right) = 158.03\, w(\tau) \frac{p \tilde{c}_t}{Z} \frac{\partial p}{\partial t} \quad (14)$$

$$\tilde{\mu} = \frac{\mu(p)}{\mu_i} \quad (15)$$

$$\tilde{c}_t = \frac{c_t(p)}{c_{ti}} \quad (16)$$

where,

Z, compressibility factor;

$w(\tau)$, derivative of drainage volume w.r.t diffusive time of flight;

$\tilde{\mu}$, dimensionless viscosity;

$\tilde{c}_t$, dimensionless total compressibility;

μ_i, viscosity at initial pressure (cp);

c_{ti}, total compressibility at initial pressure ($psia^{-1}$);

Eq. (14) is final form of 1-D diffusivity equation for gas using diffusive time of flight. 1-D solution has now been extended for a dual porosity system; this will be used for case studies in the following chapters.

2.3 1-D Pressure/Rate Solution for a Dual Porosity Model

For shale models we have accounted for a dual porosity system, rock compaction and additional immobile phase (irreducible water in this case). For this case we have two mass balance equations; one for Fractures and other one containing matrix. In this type of system, matrix acts as the storage for hydrocarbons and fracture alone act as conduit responsible for production.

Mass balance equation for fracture is given by **Eq. (15)** and **Eq. (16).** Fluid properties in the transfer function subscripted as "up" are evaluated at upstream direction (upwinding).

$$\nabla \cdot \left(\frac{\rho}{\mu} k \nabla p\right) = \frac{\partial(\rho\phi)}{\partial t} + \rho_{up}\Gamma \quad \ldots\ldots\ldots\ldots\ldots\ldots\ldots\ldots\ldots\ldots \text{(15)}$$

$$\Gamma = \sigma \frac{k_m}{\mu_{up}} \left(p_f - p_m\right) \ldots\ldots\ldots\ldots\ldots\ldots\ldots\ldots\ldots\ldots\ldots \text{(16)}$$

where,

Γ, transfer function between fracture and matrix (defined by Kazemi's equation);

k_m, matrix permeability;

ρ_{up}, fluid density (calculated by upwinding scheme);

μ_{up}, fluid viscosity (calculated by upwinding scheme);

σ , geometric shape factor (modeled by the Gilman & Kasemi model or Warren & Root model);

p_f, fracture pressure;

p_m, matrix pressure;

Substitute **Eq. (16)** in **Eq. (15)** and apply chain rule. Now substitute ρ_{up} using equation of state of gas (real gas law) and rearrange and replace rock and gas compressibility for total compressibility. Then using divergence theorem, to transform the equation in 1-D coordinates we get **Eq. (17)** and **Eq. (18).**

$$\frac{\partial}{\partial \tau}\left(w(\tau) \frac{p_f}{\tilde{\mu} Z} \frac{\partial p_f}{\partial \tau}\right) = w(\tau) \frac{p_f \tilde{c}_t}{Z} \frac{\partial p_f}{\partial t} - v(\tau) \frac{1}{c_{ti}} \left(\frac{p}{\mu Z}\right)_{up} \sigma k_m \left(p_f - p_m\right) \ldots\ldots\ldots \text{(17)}$$

$$v(\tau) = \frac{w(\tau)}{\phi} \ldots\ldots\ldots\ldots\ldots\ldots\ldots\ldots\ldots\ldots\ldots\ldots\ldots\ldots \text{(18)}$$

where,

$v(\tau)$, derivative of the bulk volume with respect to τ

The shape factor is modeled by the Gilman and Kasemi method or Warren and Root method, which assume the pseudo-steady state condition within a matrix grid. Mass balance for matrix is given in **Eq. (19).**

$$\frac{\partial(\phi_m \rho_m)}{\partial t} - \rho_{up}\Gamma = 0 \quad \ldots\ldots\ldots (19)$$

where,

ϕ_m , matrix porosity;

ρ_m , gas density at matrix condition;

Final form of mass balance equations on 1-D coordinates in field units for fracture and matrix is given by **Eq. (20)** and **Eq. (21)** respectively.

$$\frac{\partial}{\partial \tau}\left(w(\tau)\frac{p_f}{\tilde{\mu} Z}\frac{\partial p_f}{\partial \tau}\right) = 158.03\, w(\tau)\frac{p_f \tilde{c}_t}{Z}\frac{\partial p_f}{\partial t} - v(\tau)\frac{1}{c_{ti}}\left(\frac{p}{\mu Z}\right)_{up}\sigma \quad \ldots\ldots\ldots (20)$$

$$158.03\rho_m \phi_m c_{tm}\frac{\partial p_m}{\partial t} - \rho_{up}\sigma\frac{k_m}{\mu_{up}}\left(p_f - p_m\right) = 0 \quad \ldots\ldots\ldots (21)$$

where,

c_{tm} , total compressibility in matrix;

In **Eq. (20)**, we have flux term followed by accumulation term and transfer function. For matrix (storage) mass balance equation we only have accumulation term and transfer function.

The rock compaction effect can be modeled using variable porosity and permeability as a function of pressure **Eq. (22)**.

$$c_t = c_g + \left(\frac{1}{M_\phi}\right)\left(\frac{dM_\phi}{dp}\right) \ldots\ldots\ldots\ldots\ldots\ldots\ldots\ldots\ldots\ldots\ldots\ldots\ldots\ldots\ldots\ldots\ldots\ldots\ldots\ldots\ldots\ldots\ldots\ldots\ldots (22)$$

where,

M_k , permeability multiplier;

M_ϕ , porosity multiplier;

In addition, in the presence of irreducible water saturation S_{wi}, the net pore volume occupied by mobile gas phase becomes $(1-S_{wi})\phi$. Then the following comprehensive equations **(Eq. (23) & Eq. (24))** can be derived:

$$\frac{\partial}{\partial\tau}\left(w(\tau)\frac{P_f M_k}{\tilde{\mu}z}\frac{\partial P_f}{\partial\tau}\right) = w(\tau)(1-S_{wif})\frac{\tilde{c}_t P_f}{z}\frac{\partial P_f}{\partial t} + w(\tau)\frac{1}{\phi_i c_{ti}}\left(\frac{P}{\mu z}\right)\Gamma \ldots\ldots\ldots\ldots\ldots\ldots\ldots (23)$$

$$\left(\frac{P_m}{\mu z}\right)(1-S_{wim})\phi_m c_{tm}\frac{\partial P_m}{\partial t} = \left(\frac{P}{\mu z}\right)_{up}\Gamma \ldots\ldots\ldots\ldots\ldots\ldots\ldots\ldots\ldots\ldots\ldots\ldots\ldots\ldots\ldots\ldots\ldots\ldots (24)$$

where,

S_{wif}, irreducible water saturation in fracture;

S_{wim} , irreducible water saturation in matrix;

2.4 Synthetic Case Study

This section presents an example case study to show the capability of fast marching method. This case study is a modified version of a dual porosity model of the example presented by Zhang et al. (2013). **Table 1** lists the details of property distribution in the model. **Figure 2 (a)** and **Figure 2 (b)** show the fracture permeability distribution and locations of fracture stages along the well trajectory respectively. **Figure 3** shows the porosity distribution in the fracture system. For diffusive time of flight calculations; constant values of compressibility and viscosity are used as 1.43×10^{-4} $psia^{-1}$ and 0.024cp.

Table 1: Parameters used in the synthetic example

Parameter	Value
Grid dimension	2.4 million cells
Matrix permeability	$k_x = k_y$ = 0.0001md; k_z = 0.00001md
Fracture permeability	1 nd – 1.05 md
Matrix porosity	0.1
Fracture porosity	$4 \times 10^{-6} – 9.72 \times 10^{-2}$
Hydraulic fracture permeability	$k_x = k_y$ = 10md; k_z = 1md

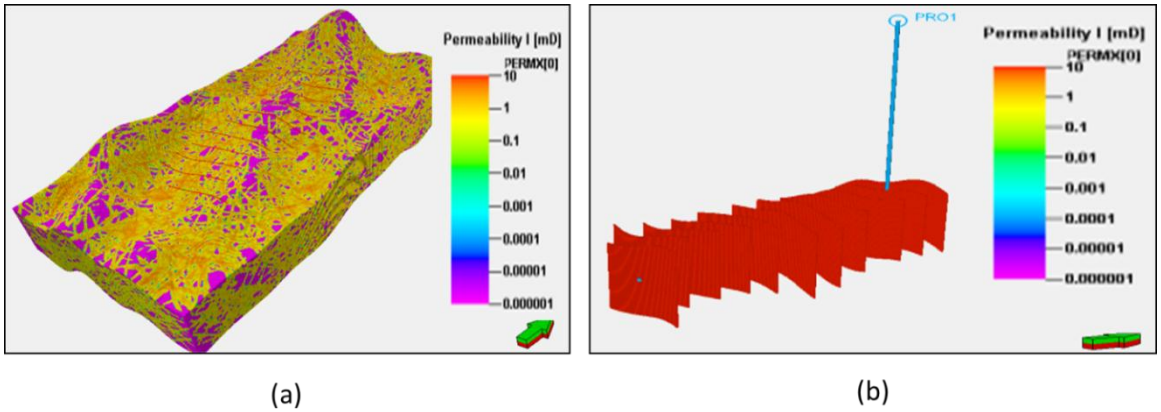

(a) (b)

Figure 2: (a) Fracture permeability (md) map (b) Hydraulic fracture locations along well trajectory on a permeability map

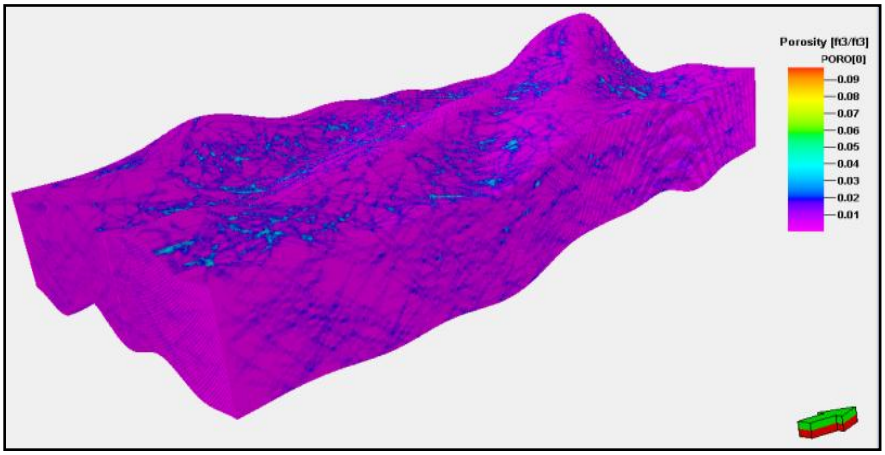

Figure 3: Fracture porosity map

Diffusive time of flight is calculated using corner point geometry algorithm for fast marching method. Based on time of flight values, 1-D pressure/rate solution equations are put to application as per section 2.1. We have two cases in consideration.

Case A has the production constraint as flowing bottom hole pressure (BHP) and we will compare gas rate output from a commercial finite difference simulator (FDSIM) and 1-D solution. The well is produced according to the **Table 2**:

Table 2: Case A production constraint table

Time, days	BHP, psia
1080	4500
1080	3000
1800	2000

Case B has the production constraint as gas rate and we will compare flowing bottom hole pressure output from FDSIM and 1-D solution. The well is produced according to the Table 3:

Table 3: Case B production constraint table

Time, days	Gas Rate, Mscf/d
1080	663
1080	473
1800	284

For the model discussed in this section, we first calculate diffusive time of flight and thereafter implimenting1-D pressure/rate solution on the time of flight for the two production constraints. Figure 4 and Figure 5 are the results obtained from the comparison study.

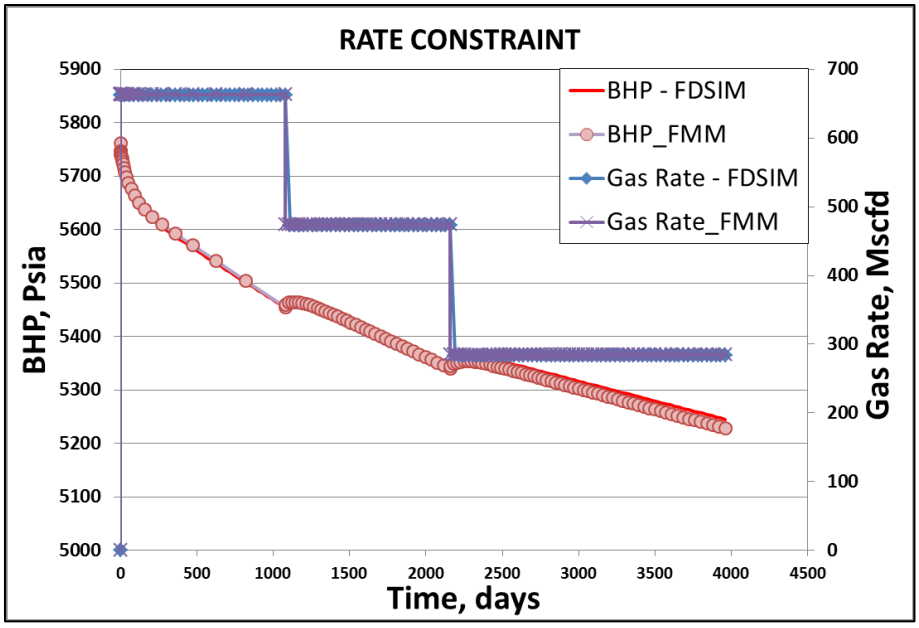

Figure 4: Case A - Comparison plot for FDSIM and 1-D solution (FMM) results for well gas rate with flowing bottom hole pressure as constraint

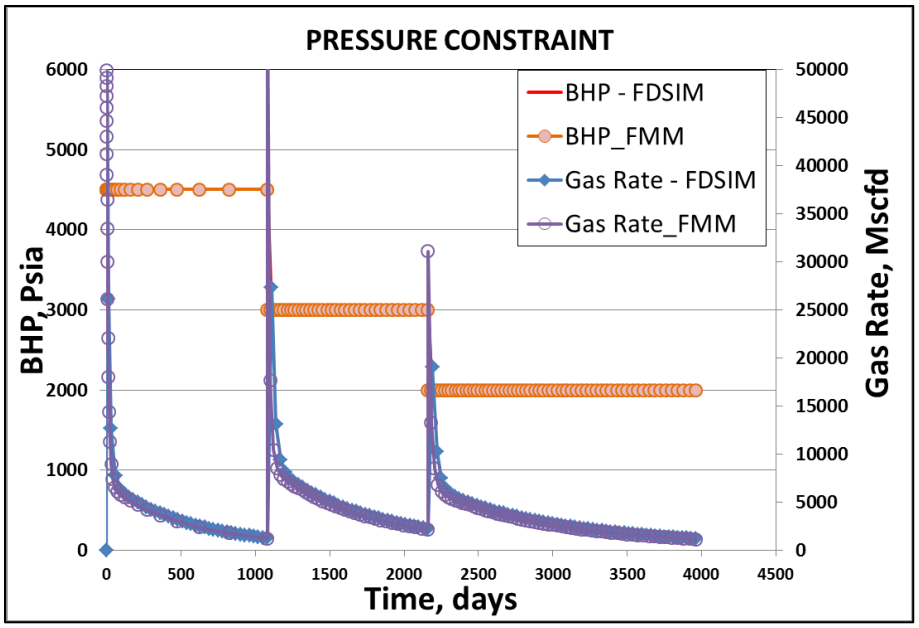

Figure 5: Case B - Comparison plot for FDSIM and 1-D solution (FMM) results for well flowing bottom hole pressure with gas rate as constraint

The comparison plots for both the cases show that the solutions from a commercial simulator matches reasonably well with output from FMM using 1-D solution. One of the main benefits of using FMM method is considerable saving in computation time.

Table 4 shows a run time comparison between FDSIM and FMM:

Table 4 : Run time comparison between FD simulator and Fast Marching Method

Method	Run Time, Minutes
FDSIM	129
DTOF+1-D solution	<5

Table 4 clearly shows for this case, fast marching method is ~twenty times faster than a commercial simulator.

Through this work and previously reported work, FMM is proven to have a number of advantages over analytical and numerical solutions. Unlike analytical methods, fast marching method can be applied using complex grid geometry (corner point) and heterogeneous property distribution (permeability, porosity). This method does not need to work on the assumption of constant rate or constant pressure wellbore condition, which is basis for methods like decline curve analysis.

In comparison to full field simulation approach, FMM requires lesser data and can do the calculation and visualization of drainage volume in a much shorter duration for even a multi-million cell model. As supported in the literature, FMM can act as an evaluation tool for model parameters, data collection and even a preliminary tool for history matching before moving on to full field numerical simulation study. Taking this background, we will present the field case study.

CHAPTER III

ANADARKO CASE STUDY

This chapter includes details of the field data for a shale gas reservoir located in East Texas, USA. Data for this study has been provided by Anadarko Petroleum Corporation (APC). Production data (~ 450 days), has been used to perform a rate transient analysis, details of the same has been discussed in this chapter.

3.1 Data Description

Data set provided by APC includes the following:

1. Grid definition
    a. corner point geometry
    b. reservoir properties(permeability, porosity and saturation distribution)
2. Completions data:
    a. hydraulic fracture job summary
    b. wellbore schematic
3. Properties
    a. hydraulic fracture properties (fracture size – base values, stimulated reservoir volume – base values)
    b. fracture spacing
    c. rock compaction table
    d. relative permeability tables

4. PVT - compositional model details
5. Production
    a. well flow back data
    b. daily production for ~450days

3.2 Model Description

The model has one horizontal well with twenty two stages of hydraulic fractures. Since a seismic study was not conducted on this field, hence well logs were mostly relied on for reservoir property distributions like porosity and permeability. The base model can also be described as a layer cake model i.e. mostly vertical heterogeneity can be observed and not areal heterogeneity.

Grid dimensions of the base model are 41x71x16 cells. A visual inspection of approximate grid block sizes suggests that the model is very coarse. A grid top view with the horizontal well placement can be seen in **Figure 6**. Reservoir property distribution map of the reservoir show the Stimulated Reservoir Volume (SRV) definition. It may be noted that all the hydraulic fracture definitions have been made along the wellbore trajectory as shown in **Figure 7**. SRV region has been modeled with an inner SRV region containing fracture stages and outer SRV region shown as SRV boundary. The minimum SRV width and thickness are based on hydraulic fracture definition. Whereas maximum SRV width equals ± three grid blocks from fracture

location and maximum thickness covers all sixteen layers in the model, as shown in **Figure 7** and **Figure 8** respectively.

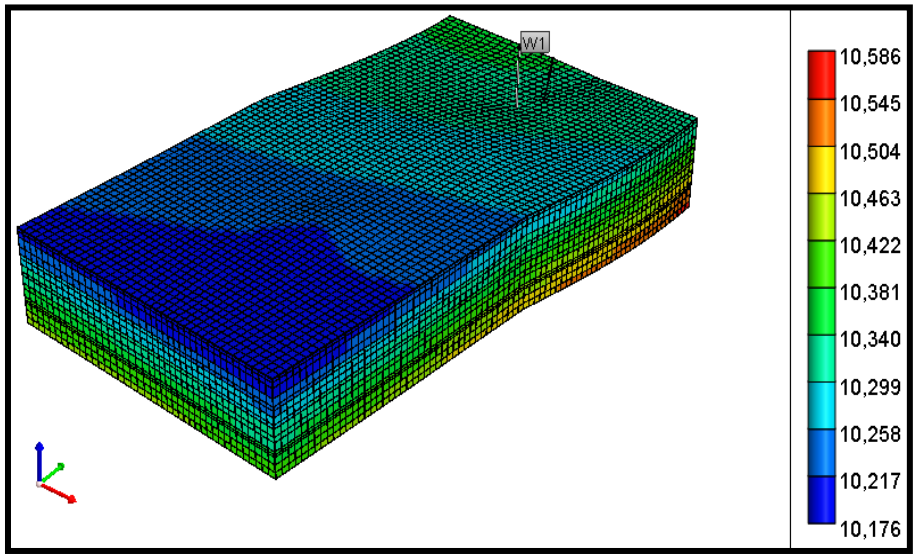

Figure 6: Grid top (ft) 3D view with horizontal well placement

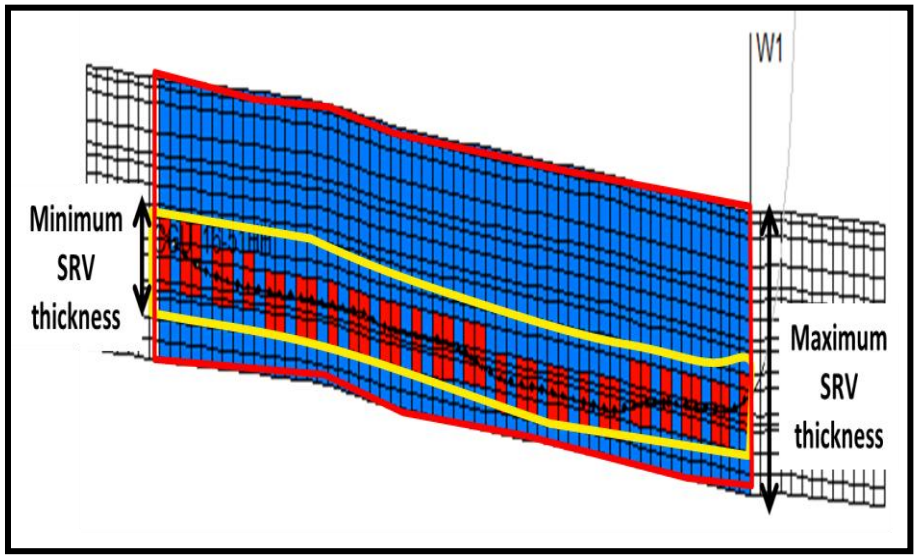

Figure 7: JK cross-section of permeability distribution map

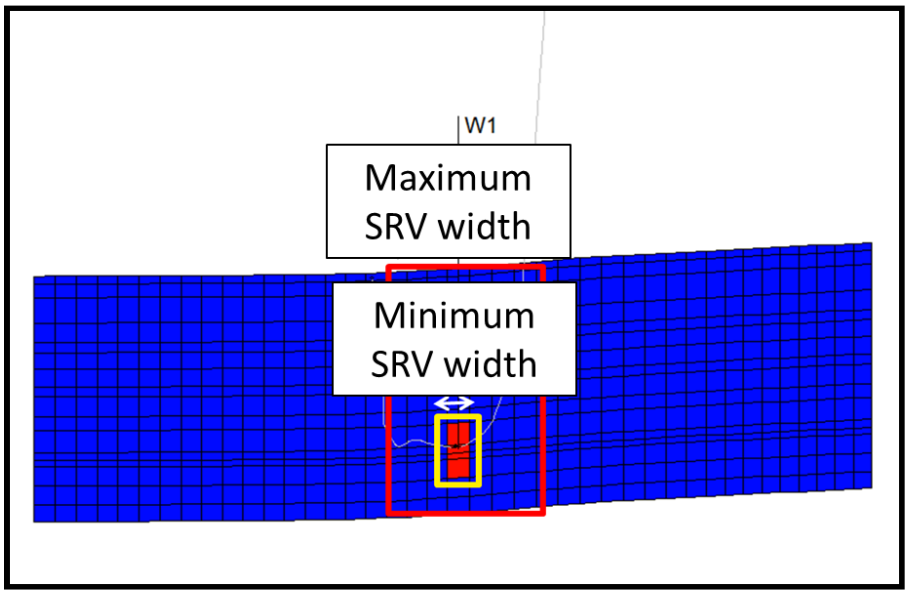

Figure 8: IK cross-section of permeability distribution map

The reservoir property distributions such as porosity, permeability and saturations will be discussed in the History Matching (HM) section in detail.

3.3 Production Data Analysis

Kabir et al. (2011) pointed out that in most tight reservoirs there are two most dominant flow regimes seen:

1. Linear flow regime characterized by half slope line on a log-log plot
2. Transitional period a signature of apparent bounded volume, characterized by ~unit slope line on a log/log plot.

Transitional period; as the name suggests is a transition to compound liner flow regime from a linear flow regime. The apparent bounded volume arises because of fracture stage interference.

In Anadarko case study, the production data analysis has been done using the ~450 days gas rate production data and casing head pressure data is available from 127days from start of production. Casing head pressure was converted to bottom hole pressure conditions based on wellbore trajectory. KAPAA Company's rate transient analysis software TOPAZ has been used for production data analysis.

A history matching on production data was done (discussed in CHAPTER IV). For the purpose of history matching, gas rate as a constraint was used for first 126 days of production and calculated bottom hole pressure for remaining number of days.

Since we didn't have pressure data for some part of production history, hence the history match prediction of bottom hole pressure for 127 days of production was used for production data analysis.

3.3.1 Input Data

Figure 9 shows the plot of input data of gas rate and flowing bottom hole pressure used for the rate transient analysis.

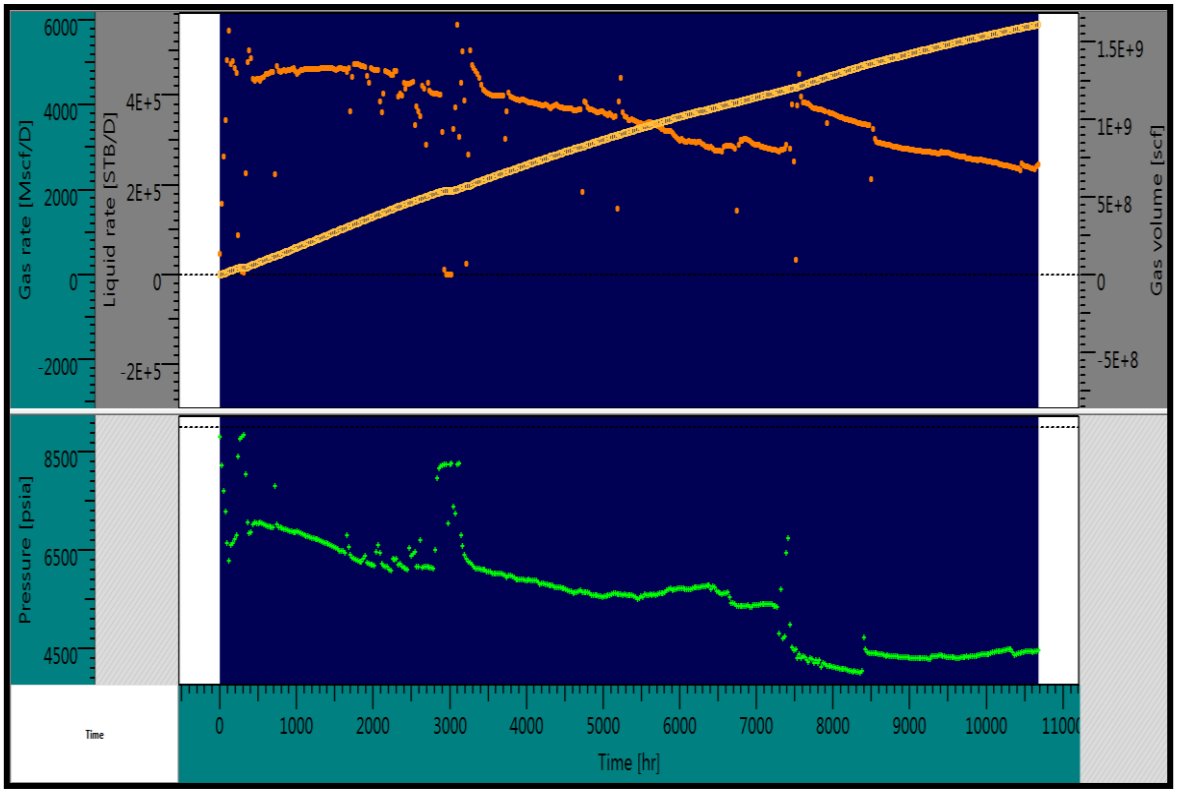

Figure 9: Input data for well gas rate, gas cumulative rate and bottom hole pressure values for rate transient analysis

3.3.2 Flow Regimes

Using TOPAZ (rate transient analysis software by Kappa) a normalized pressure integral plot is used to identify various flow regimes in data. **Figure 10** identifies a unit slope line, which is a signature of an apparent bounded volume called SRV (stimulated reservoir volume).

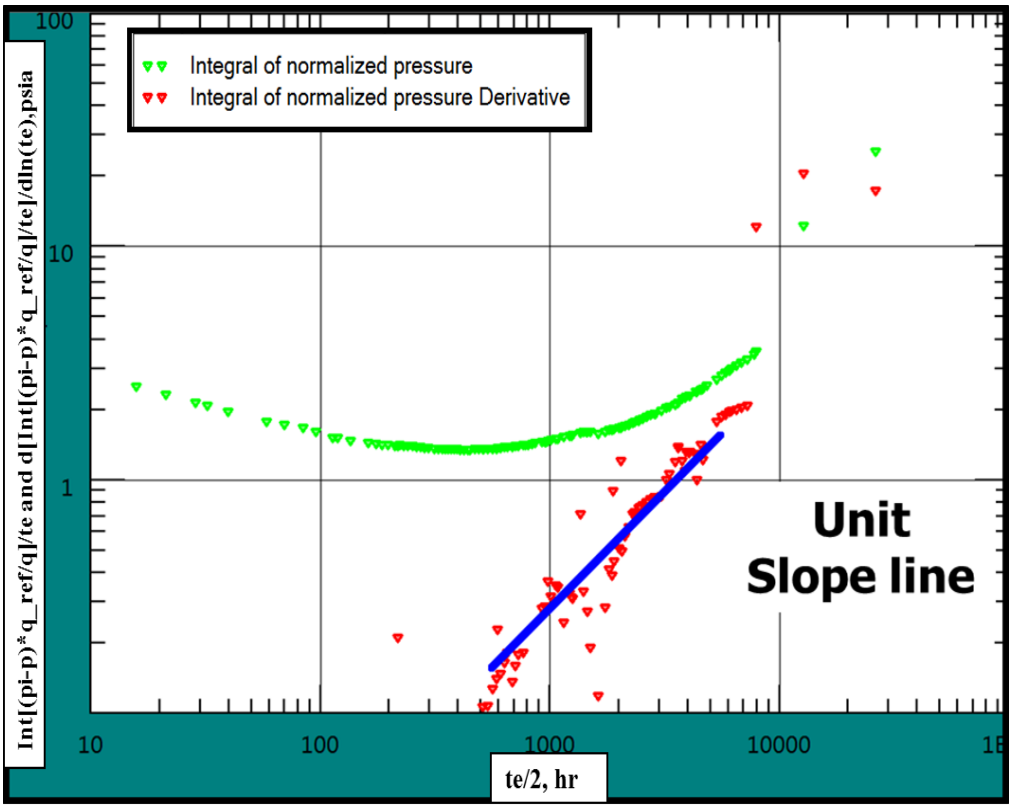

Figure 10: Normalized pressure integral plot

It may be noted that pressure data for first 127 days was missing, hence history matched simulation results for bottom hole pressure values was used. Based on permeability values and other reservoir properties, initial flow regimes associated with fractures, like linear flow and bilinear flow would have passed in missing pressure data. However, at hand data can be used to calculate an approximate SRV and reservoir properties like permeability, skin fracture conductivity etc.

3.3.3 Model Selection

Based on information in the model description section of this chapter, a horizontal well with finite conductivity hydraulic fractures is chosen as the base model. The flow regimes identified in the normalized pressure integral plot suggests that a bounded volume needs to be considered in the model. A rectangular closed system model is considered with a horizontal well and finite conductivity fractures.

Figure 11 and **Figure 12** show normalized pressure integral and Blasingame plots with matched results. **Figure 13** is a summary plot to show the matched data comparison with the input pressure and rate data.

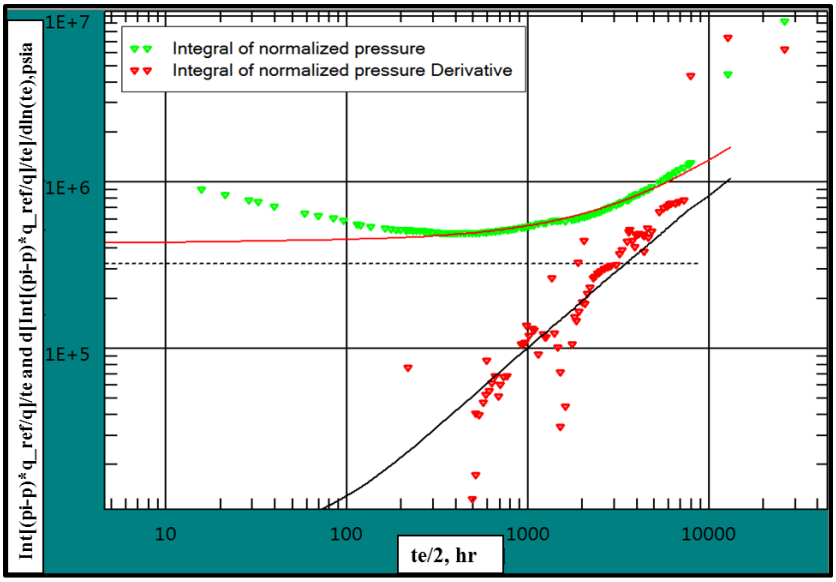

Figure 11: Normalized pressure integral plot with matched results

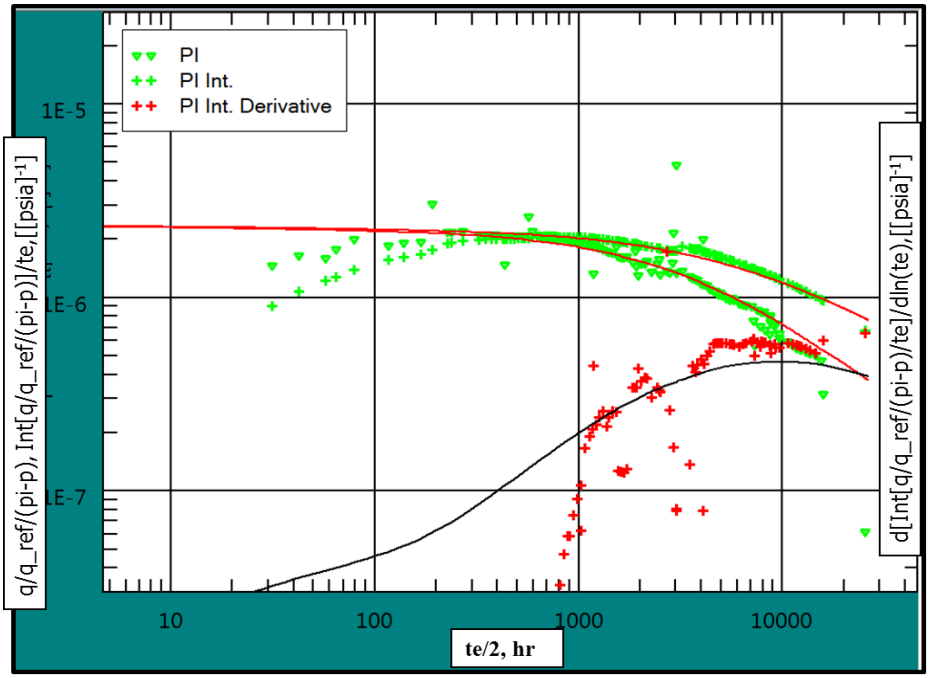

Figure 12: Blasingame plot with matched results

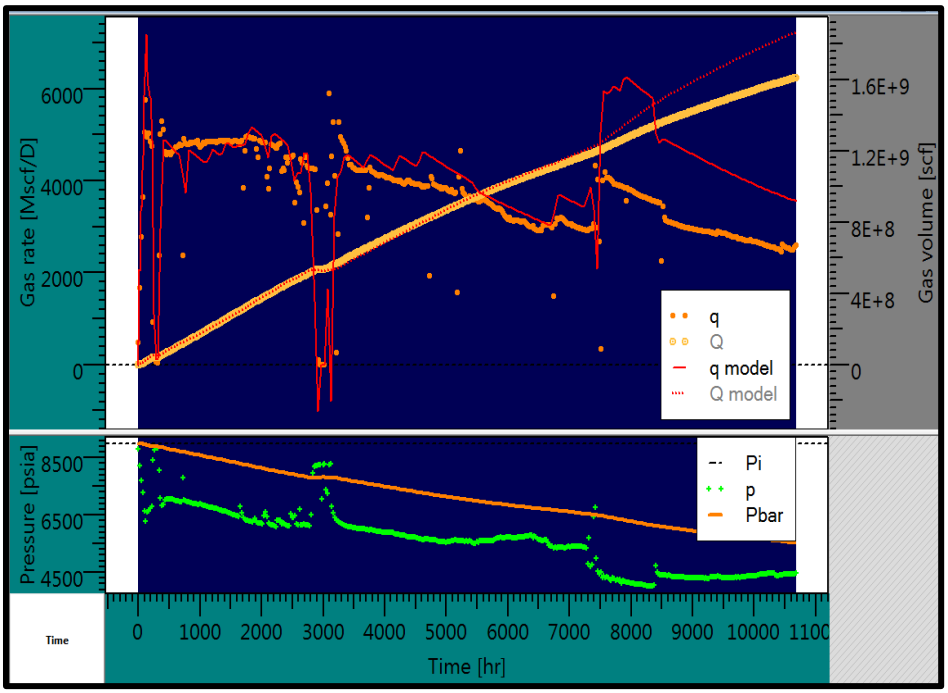

Figure 13: Matched results for well gas rate, gas cumulative rate and bottom hole pressure values for rate transient analysis

In **Figure 12** and **Figure 13** solid black and red lines represent the matched model output. Also the following terms are used to represent axis in both normalized pressure integral plot and Blasingame plot.

where,

t_e, equivalent time;

q, gas rate;

q_ref, reference gas rate;

p_i, initial pressure;

p, pressure;

All the above plots show reasonable match to the history data; especially for normalized pressure integral and Blasingame plot. Towards the end of **Figure 13**, we can see that, the match doesn't hold very well. A number of factors like rock compaction and adsorption could be influencing this part of match. Non-linear module in the software allows the use of these additional parameters such as rock compaction, adsorption etc. but is only applicable for a numerical study. We have restricted this part of study solely to an analytical analysis. It may be noted that, rock compaction has been accounted for, during the history matching part and we will be able to notice a considerable improvement in match in that section.

3.3.4 Results

The well in consideration has perforation clusters (8 per fracture stage); hence numbers of fractures used is more than fracture stages. For pay thickness, the full simulation model thickness has been considered. Average value of water saturation has been considered. **Eq. (22)** and **Eq. (23)** are used to calculate the values of omega and lambda in the dual porosity model.

$$\omega = \frac{(\varphi\, c_t\, h)_{fracture}}{(\varphi\, c_t\, h)_{fracture} + (\varphi\, c_t\, h)_{matrix}} \quad \ldots\ldots (22)$$

$$\Lambda = \alpha \frac{k_2}{k_1} \quad \ldots\ldots (23)$$

where,

ω, storativity ratio;

Λ, interporosity flow coefficient;

h, pay thickness (ft);

α , shape factor;

k_1, fracture permeability;

k_2, matrix permeability;

Table 5 shows list of parameters used for analytical history match.

Table 5: Rate transient analysis result table

PARAMETER	VALUE
Well length, ft	6000
Number of fractures	176
Fracture half length, ft	100
Pay thickness, ft	240
Permeability, md	4.17 E-3
Skin	0.14
SRV dimension, ft	400 x 6100
Omega	1.43 E-1
Lambda	5.37 E-1
Water saturation, %	42
Fracture conductivity, md.ft	65
Gas in place, bscf	8.27

The values of history matched parameters from analytical study are comparable to simulation study in consecutive chapters.

CHAPTER IV

SENSITIVITY STUDY AND HISTORY MATCHING

For this shale gas reservoir APC has been doing an in-house history matching exercise and have provided to us the details of one of their base case models under evaluation. We have done two sets of studies on this model.

1. Case I - black oil simulation model based on the inputs provided, including SRV definition and dual permeability model - property distribution. Followed by a parameter sensitivity analysis and history matching of production data.
2. Case II – redo the SRV definition and property distribution based on a detailed parameter sensitivity study followed by history matching of production data.

This section gives a step by step detail of the Case I and II model generation, sensitivity study and history matching results.

4.1 Case I - Model Description

This part of the study is based on parameter and model definitions as per the given data set. Case I model has been designed for a three phase black oil simulation case. Literature suggests that in naturally fractured reservoirs (e.g. shale gas), fluid modeling is done using two interconnected systems of rock matrix and fractures. Here, rock matrix provides bulk rock volume and fractures contribute on permeability front. For simulation purposes, each grid block has two types of volumes associated – matrix and fracture volume. **Table 6** shows the details of property distribution in base model. The base case

model has been used to carry out parameter sensitivity study to do a history match on the production data.

Table 6: Reservoir property distribution

Parameter	Value or Range
Grid dimension	41×71×16 = 46576 cells
Grid size	DX = DY = 100ft; DZ = 5ft~15ft
Matrix porosity	0.04 ~ 0.09
SRV fracture porosity	0.01
Matrix permeability	$\boldsymbol{k_x = k_y}$ = 0.00001md ~ 0.012md; $\boldsymbol{k_z}$ = 0.00001md ~ 0.003md
SRV permeability	$\boldsymbol{k_x = k_y = k_z}$ = 0.0316md
Hydraulic fracture permeability	$k_x = k_y = k_z$ = 0.65md
Matrix water saturation	0.25 ~ 0.60
SRV water saturation	0.2
Hydraulic fracture water saturation	0.7

4.1.1 Base Case Model Generation

A compositional model is available to us but keeping in mind the scope of this study, we decided to use black oil modeling in this case. For this type of modeling, the given compositional PVT properties needed to be converted accordingly.

4.1.1.1 Pressure-Volume-Temperature (PVT) Properties

ECLIPSE Pressure-volume-temperature analysis software (PVTi) has been used to convert the compositional PVT properties to black oil model PVT properties. Peng-

Robinson Equation of State (EOS) has been used to conduct a constant volume depletion experiment on the data to get the wet gas and dead oil properties.

4.1.1.2 Stimulated Reservoir Volume (SRV) Selection

The SRV definition for the base case model for history matching has been kept consistent with the one provided for case study. SRV region boundaries as shown in **Figure 14** with x=18:24, y=14:70 and z=1:16.

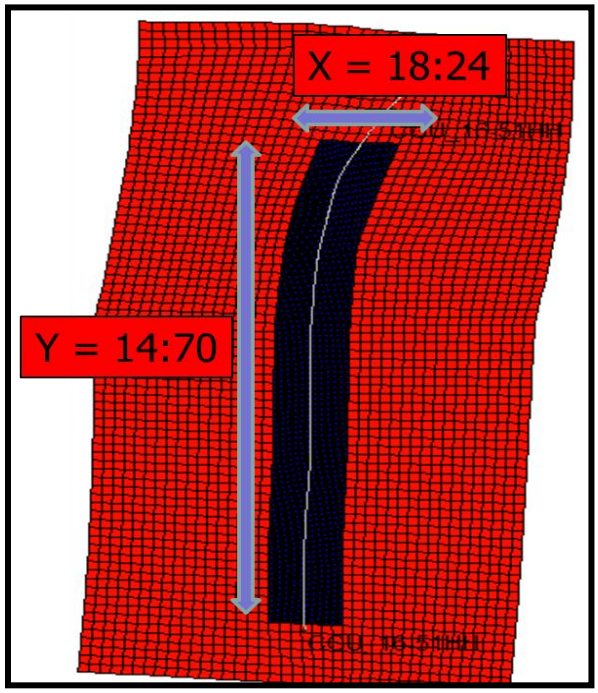

Figure 14: Areal view with SRV definition in XY direction

4.1.1.3 Dual Permeability Model

Based on reservoir property distribution, a dual permeability model has been used to represent the reservoir in this case. As mentioned before, based on the well log information the model is designed as a layer cake model with only vertical heterogeneity. Fracture permeability distribution (**Figure 15**) shows the boundaries of SRV and **Figure 16** shows the inner and outer SRV definition on the cross section map.

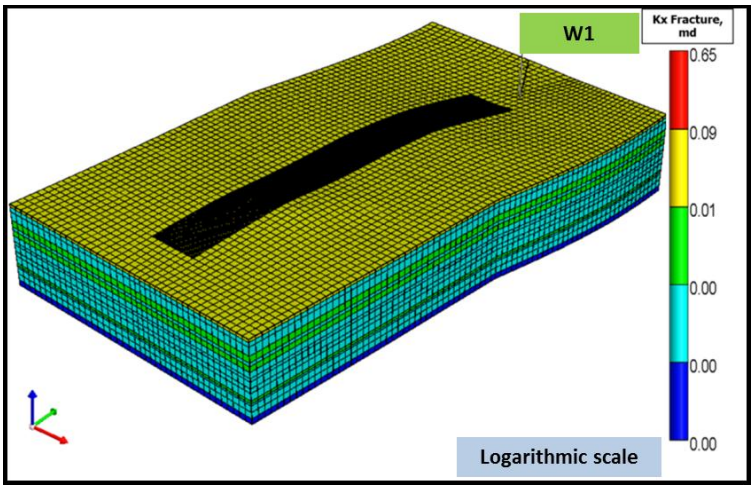

Figure 15: Areal view of x direction fracture permeability map

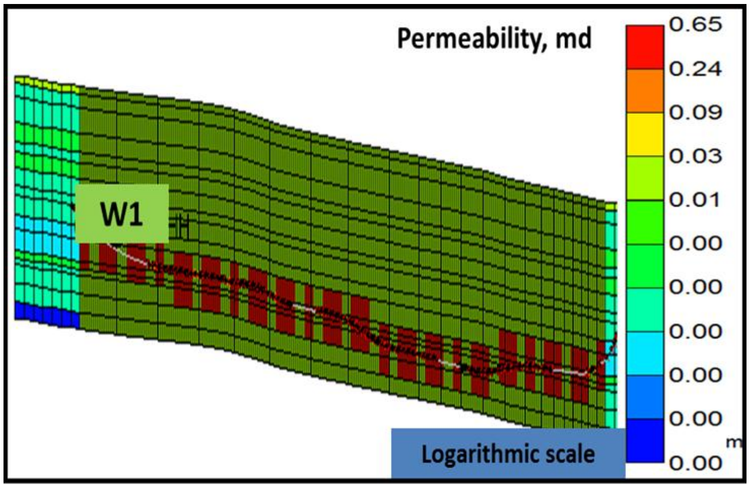

Figure 16: JK cross-section of x direction fracture permeability distribution map

4.1.1.4 Rock Compressibility and Rock Compaction

Given data set includes rock compressibility value at a reference pressure applicable to matrix system. We also have a rock compaction table applicable to fracture system. The model has been build using on a commercial finite difference simulator.

In order to include rock compressibility as well as a rock compaction table to the current case, a few changes had to be done. In order to convert rock compressibility into a compaction table, **Eq. (24)** has been used.

$$\varphi = \varphi_o \left(1 + c_r \left(p - p_o \right) \right) \ldots\ldots\ldots\ldots\ldots\ldots\ldots\ldots (24)$$

where,

$\boldsymbol{\varphi}$, porosity (fraction);

$\boldsymbol{\varphi_o}$, porosity at reference pressure (fraction);

$\boldsymbol{c_r}$, rock compressibility (psia^{-1});

$\boldsymbol{p}$, pressure (psia);

$\boldsymbol{p_o}$, reference pressure (psia);

Using this **Eq. (24)** we can get a compaction table for porosity change with change in pressure.

4.1.1.5 Shape Factor Selection

The base model has a relatively coarse grid definition .The order to reduce the grid size around the well bore region, local grid refinement has been done till the extent of SRV region.

To comprehend for a dual system, a shape factor (sigma) needs to be assigned in the model for construction of matrix-fracture coupling transmissibility. The sigma factor is defined as follows **Eq. (25):**

$$\sigma = 4 \times \left(\frac{1}{L_x^2} + \frac{1}{L_y^2} + \frac{1}{L_z^2}\right) \qquad (25)$$

where,

L_x, L_y and L_z, dimensions of matrix blocks in X, Y and Z direction (ft);

Based on above equation, two different sigma values were assigned.

1. region inside SRV
2. region outside SRV

4.1.1.6 Case I - Model Property Summary

Case I - base case model includes the following:

1. Dual permeability
2. Rock compaction(fracture) and rock compressibility(matrix)
3. Local grid refinement
4. SRV definition

It may be noted that the data set included the details for a compositional model study as well as adsorption parameters. Keeping in mind the scope of this study, we have used a black oil model with a dual permeability system. Adsorption component cannot be tracked with this case being a black oil model.

4.2 Case I - Sensitivity Study

Following the approach of Yin et al. (2011), to evaluate the impact of various parameters on production history, a set of selected parameters like permeability, porosity, water saturation and rock compaction factor have been chosen. **Table 7** shows a detailed list of selected parameters and the selected ranges for sensitivity studies.

It may be noted that, this study has been conducted assuming the SRV selection for the model is correct. Case II will deal with the production data sensitivity for SRV definition.

Table 7: Parameter uncertainties for sensitivity and history matching – Case I

Uncertainty	Base	Low	High
SRV porosity (Frac_poro), fraction	1.00E-02	1.00E-03	5.00E-02
SRV fracture permeability in x direction (kx_frac), md	3.16E-02	3.16E-04	4.11E-02
SRV matrix permeability multiplier in x direction (kx_matrix)	1	1E-02	1.3
SRV fracture permeability in z direction (kz_frac) , md	3.16E-02	3.16E-04	4.11E-02
SRV matrix permeability multiplier in z direction (kz_matrix)	1	1E-02	1.3
Hydraulic fracture permeability-x direction (kx_hyd_frac),md	6.50E-01	6.50E-03	8.45E-01
Hydraulic fracture permeability-z direction (kz_hyd_frac),md	6.50E-01	6.50E-03	8.45E-01
SRV fracture water saturation (Sw_frac), fraction	2.00E-01	2.00E-03	2.40E-01
SRV hydraulic fracture water saturation (Sw_hyd_frac), fraction	7.00E-01	7.00E-03	8.40E-01
Fracture compaction table multiplier (Frac_comp)	1	0.6	1.5
Hydraulic fracture compaction table multiplier (Hyd_frac_comp)	1	0.6	1.5

Figure 17 shows a tornado diagram of the objective function (logarithm of cumulative gas misfit) with respect to selected parameters. All these parameters have been perturbed as per the ranges in **Table 7.**

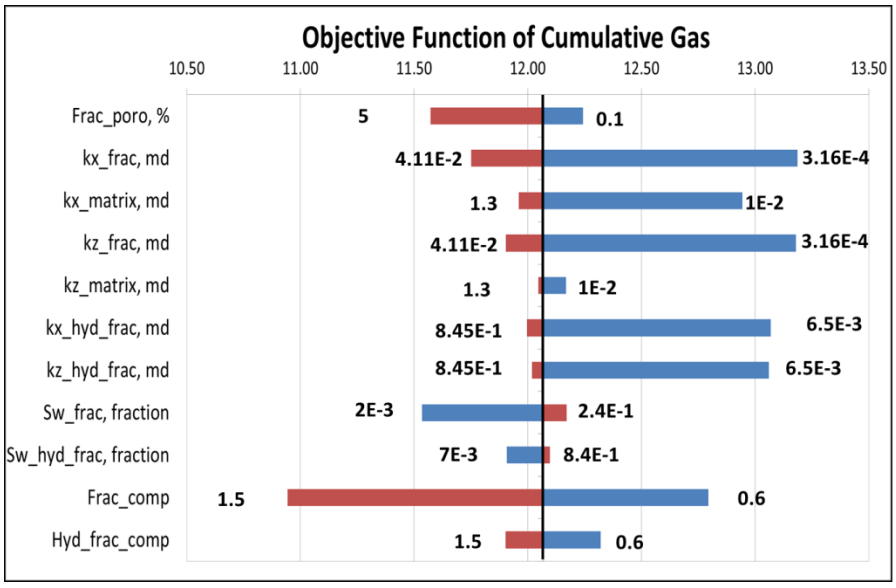

Figure 17: Tornado diagram of the objective function – logarithm of cumulative gas misfit

Tornado chart shows that the SRV fracture permeability and compaction tables have relatively more impact on the sensitivity study. Parameters having low or minimal impact on cumulative gas misfit have been dropped and set of "heavy hitters" were identified to conduct a history match on the production data.

4.3 Case I - History Matching

Based on sensitivity study as shown in previous section, the following sensitivity parameters have been chosen to do a history matching on field data:

1. Fracture porosity
2. SRV Fracture permeability – X,Z direction
3. Hydraulic fracture permeability– X,Z direction
4. SRV fracture water saturation

5. Fracture compaction table
6. Hydraulic fracture compaction table

Production history data includes:

1. Gas, water, condensate production data ~ 450 days
2. Casing and tubing head pressure 127 – 450 days

Surface pressures have been extrapolated to bottom hole conditions using a standard well flow performance software to calculate bottom hole pressure values at the kick of point of the horizontal well. For the purpose of history matching, we have used gas rate as a constraint for first 126 days of production and calculated bottom hole pressure for remaining number of days.

Comparison between history data and base case data (built based on model description section) is shown in **Figure 18(a), (b) and (c) respectively**. Using the shortlisted set of parameters in the beginning of this section, we have used Global (software by MCERI group), which is a genetic algorithm (GA) based software to conduct the history match. The software uses GA for calibrating global parameters. A proxy model is used to select from a large number of samples. Here a response surface is created by the use of experimental design after which generations are initialized. Samples which don't meet the fitness criteria are discarded and the remaining samples become part of simulations. Upon completion of a generation, if the convergence criterion is met then the final models are update locally else the proxy model is updated to continue the GA process.

Once the convergence criterion is met, the final models are locally updated to get a representative reservoir model. History match results for gas rate and cumulative production along with the bottom hole pressure are shown in **Figure 19(a), (b) and (c)** respectively.

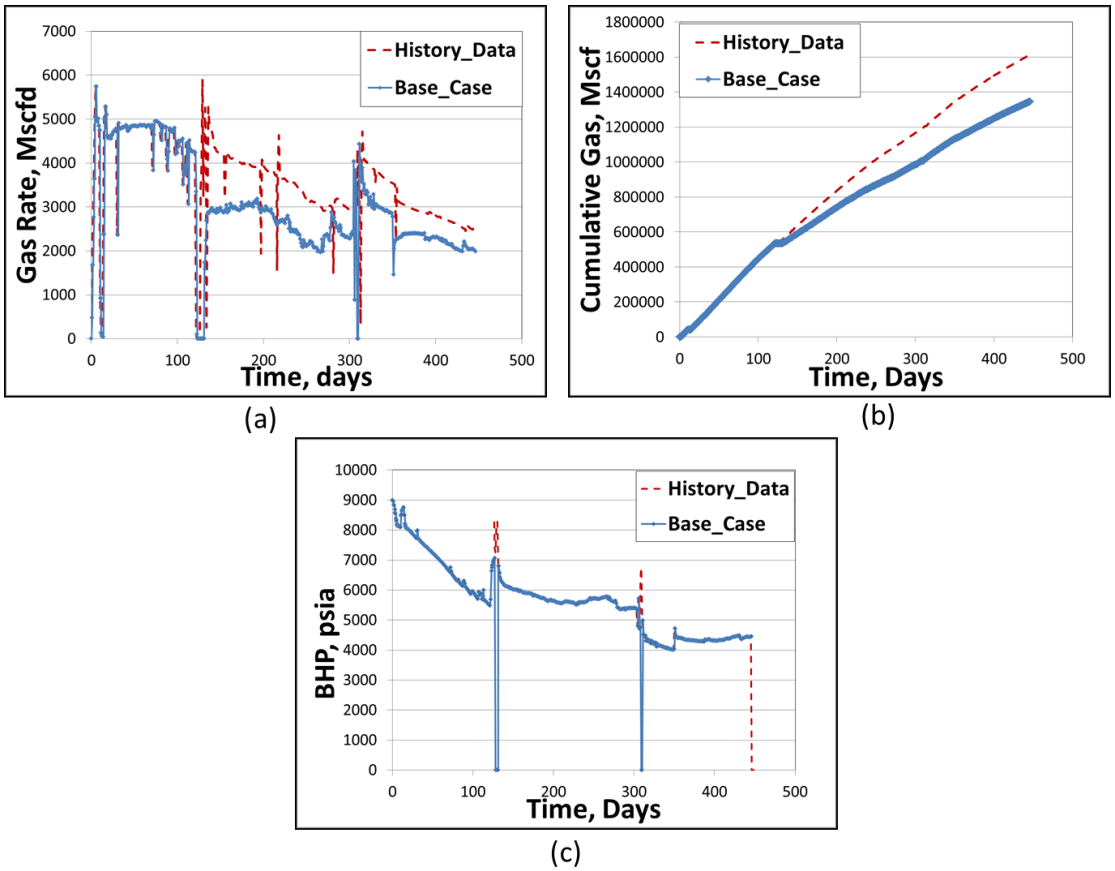

Figure 18: Comparison plot history data vs. base model output (a) Gas production rate (b) Cumulative gas production (c) Bottom hole pressure

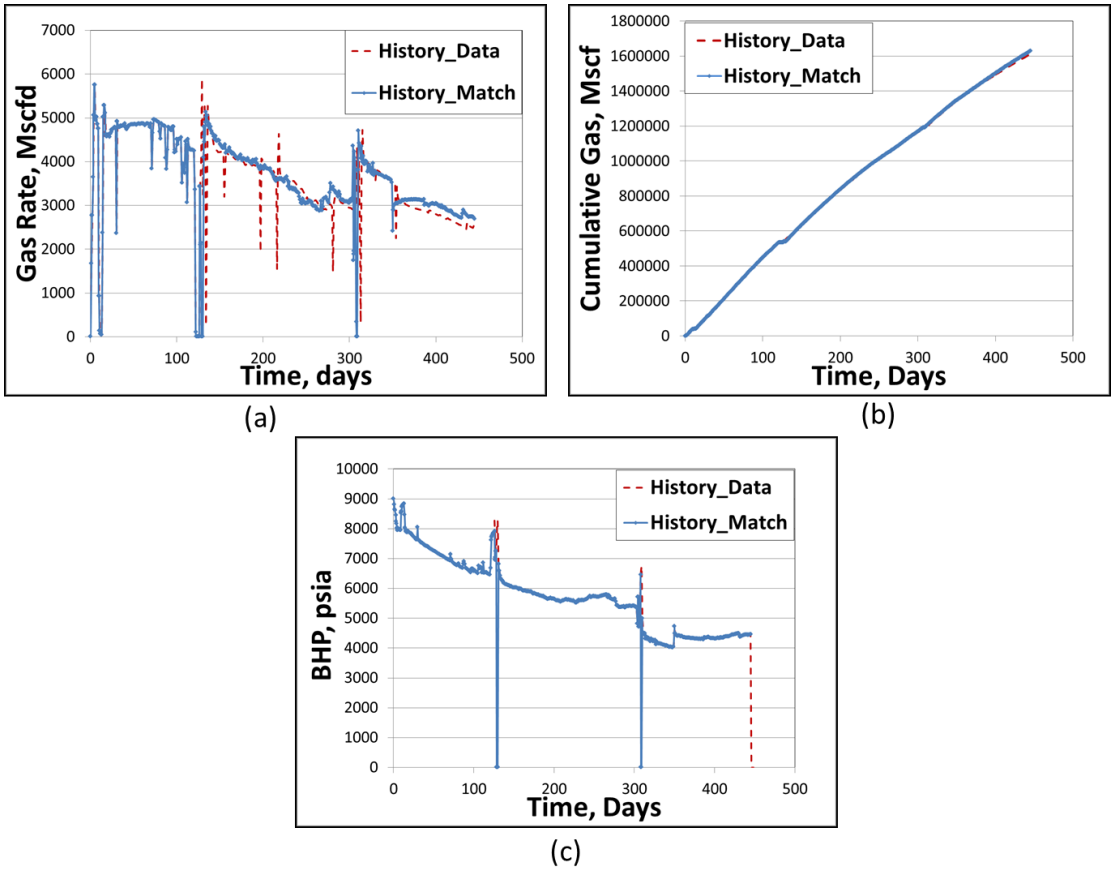

Figure 19: Comparison plot history data vs. history matched model (a) Gas production rate (b) Cumulative gas production (c) Bottom hole pressure

The comparison plots above show a good match between history data and matched model.

Figure 20(a) and (b) show the effect of history matching cumulative gas production data in the case study for reducing the parameter uncertainties. All the parameter ranges have been normalized to keep range between zero and unity. The range of every parameter is contained in the green and red box. Clearly after history matching for most of the parameters, population range is tightened to a certain extent.

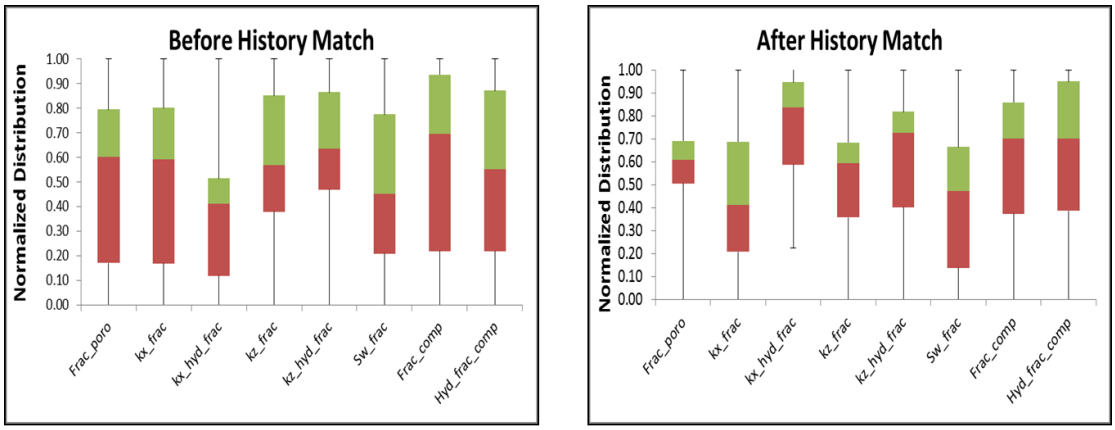

Figure 20: Uncertainty analysis of model by genetic algorithm (a) Before history match (b) After history match

4.4 Case II - Model Description

This part of the study is mostly based on parameter and model definitions as per the given data set. The main difference between Case I and Case II is that the SRV and hydraulic fracture definition is based on sensitivity study and not the given data set alone. Case II model is also black oil model with details as per following sections.

4.4.1 Stimulated Reservoir Volume (SRV) and Hydraulic Fracture Definition

The well is completed with twenty two stages of transverse hydraulic fractures. In this study the fracture and SRV dimensions have been defined as per **Figure 21**. For Case II study, the fracture locations have been kept same as in Case I. Also each fracture is considered to be surrounded by an SRV that contains natural/hydraulic fracture induced permeability enhancements. For the purpose of property distribution and sensitivity study, SRV region has been divided into four groups as per **Figure 22**.

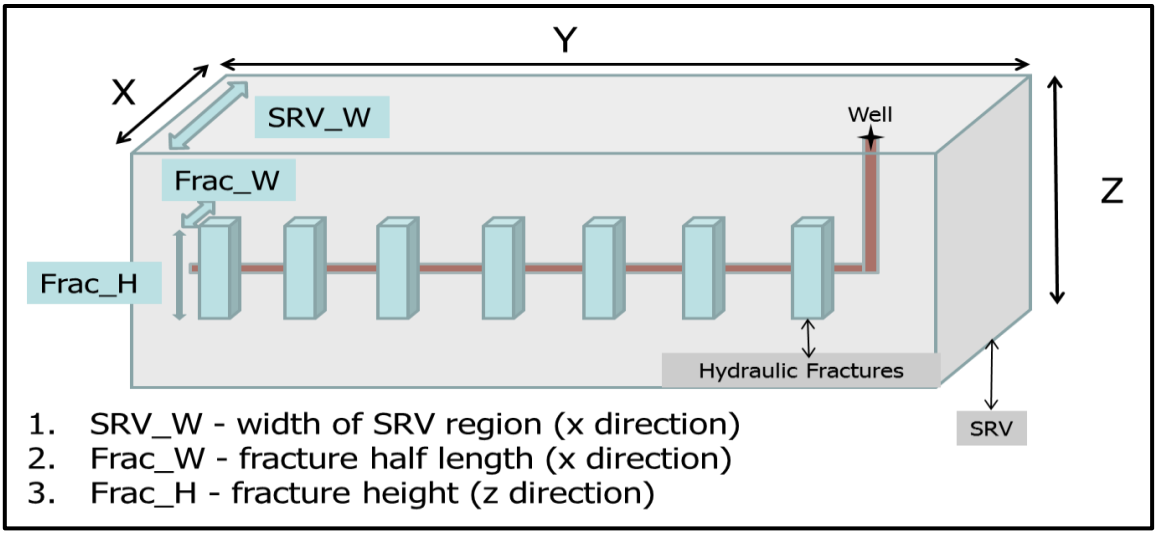

Figure 21: Hydraulic fracture and SRV definition setup for sensitivity study

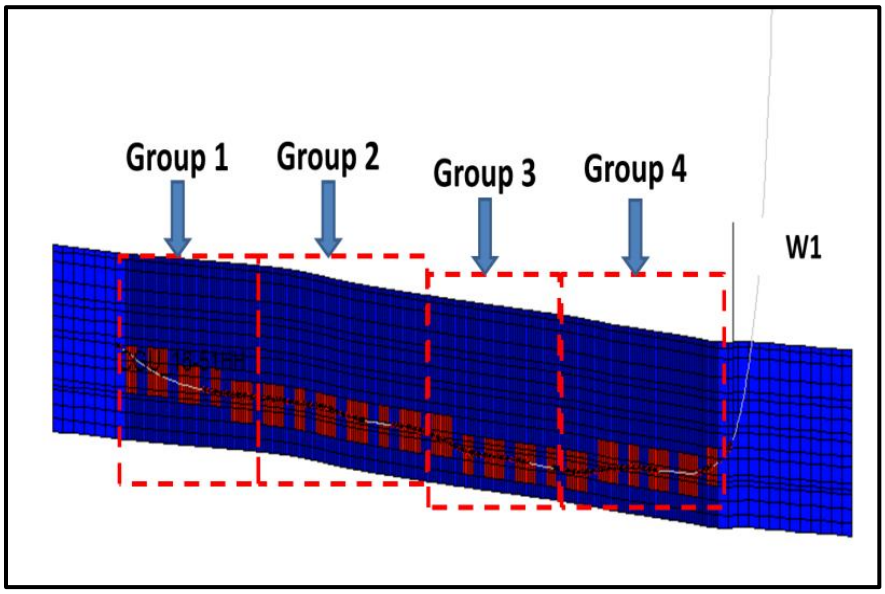

Figure 22: Group definition for sensitivity study

Following properties inside SRV and hydraulic fractures are grouped in four parts:

1. Fracture and hydraulic fracture permeability
2. Fracture porosity

3. Fracture and hydraulic fracture water saturation

All the other properties and reservoir geometry, including rock compaction, rock compressibility, matrix porosity and permeability distribution are based on Case I.

4.5 Case II - Sensitivity Study

Table 8 shows a detailed list of selected parameters and the selected ranges for sensitivity studies.

In this case study SRV and fracture definition are the additional sensitivity parameters to other reservoir properties such as permeability, porosity, water saturation and rock compaction.

Table 8: Parameter uncertainties for sensitivity and history matching – Case II

Uncertainty Parameter (variables defined)	Base	Low	High
SRV fracture porosity (Frac_poro1, Frac_poro2, Frac_poro3, Frac_poro4)	0.01	0.001	0.05
SRV fracture permeability in x direction, md (kx_frac1, kx_frac2 , kx_frac3, kx_frac4)	0.0316	0.000316	0.0411
SRV hydraulic fracture permeability in x direction, md (kx_hyd_frac1, kx_hyd_frac2, kx_hyd_frac3, kx_hyd_frac4)	0.650	0.0065	6.5
SRV matrix permeability multiplier in x direction, md ((kx_matrix1, kx_ matrix2, kx_ matrix3, kx_ matrix4)	1	0.01	1.3
SRV hydraulic fracture permeability in z direction, md (kz_hyd_frac1, kz_hyd_frac2, kz_hyd_frac3, kz_hyd_frac4)	0.0316	0.000316	0.0411
SRV hydraulic fracture permeability in z direction, md (kz_hyd_frac1, kz_hyd_frac2, kz_hyd_frac3, kz_hyd_frac4)	0.65	0.0065	6.5
SRV matrix permeability multiplier in z direction, md ((kz_matrix1, kz_ matrix2, kz_ matrix3, kz_ matrix4)	1	0.01	1.3
SRV fracture water saturation (Sw_frac1, Sw_frac2, Sw_frac3, Sw_frac4)	0.2	0.002	0.24
SRV hydraulic fracture water saturation (Sw_hyd_frac1, Sw_hyd_frac2, Sw_hyd_frac3, Sw_hyd_frac4)	0.7	0.007	0.84
Fracture compaction table multiplier (Frac_comp)	1	0.6	1.5
Hydraulic fracture compaction table multiplier (Hyd_frac_comp)	1	0.6	1.5
Fracture half length, ft (Frac_W1, Frac_W2, Frac_W3, Frac_W4)	150	50	250
Fracture height, ft (Frac_H1, Frac_H2, Frac_H3, Frac_H4)	60	30	90
SRV width, ft (SRV_W1, SRV_W2, SRV_W3, SRV_W4)	350	250	650

Figure 23(a) and (b) show tornado diagrams of the objective function logarithm of cumulative gas misfit) with respect to selected parameters. All these parameters have been perturbed as per the ranges in **Table 8**.

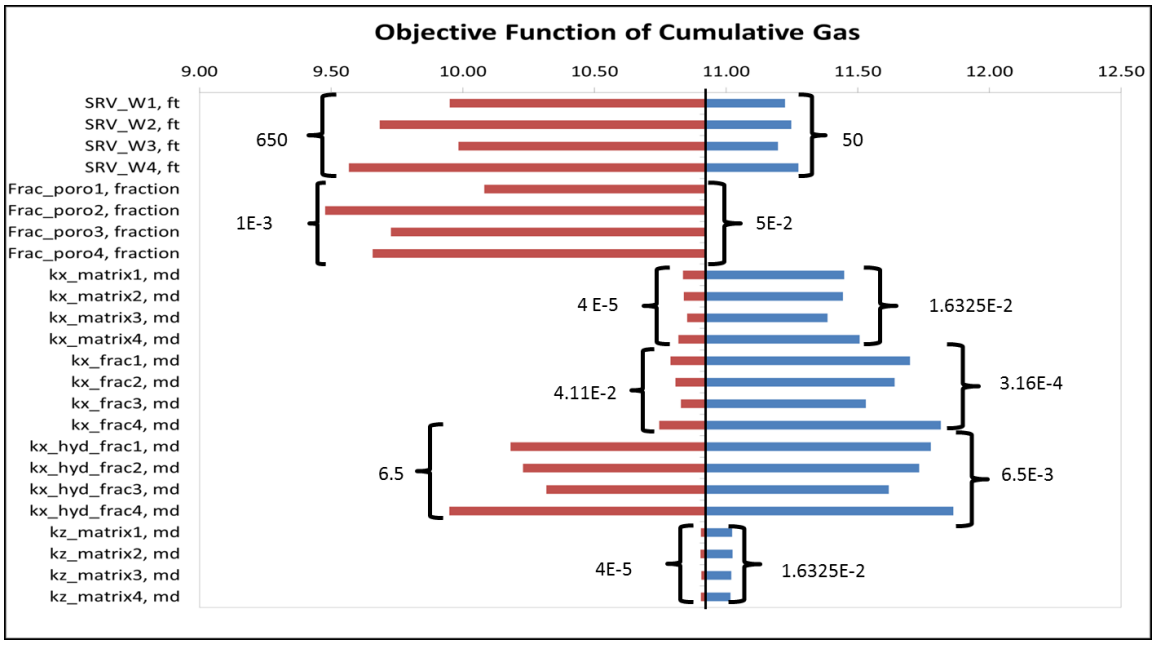

(a)

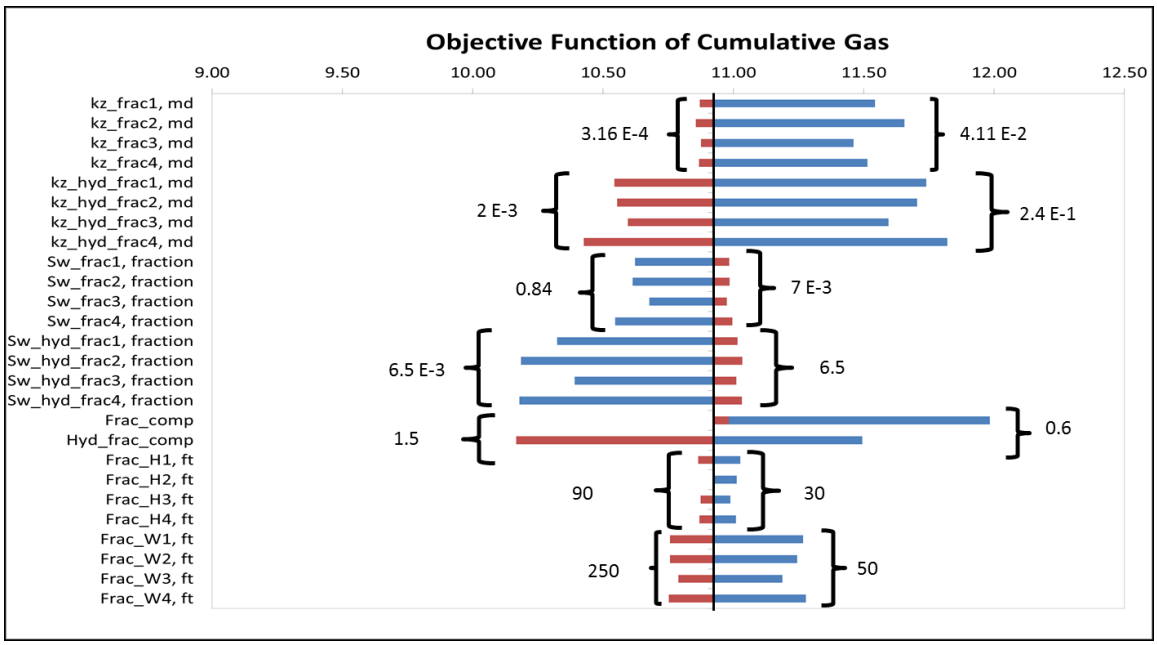

(b)

Figure 23(a), (b): Tornado diagrams of the objective function – logarithm of cumulative gas misfit

From the tornado diagrams it can be seen that SRV and fracture size has a major impact on cumulative gas misfit along with SRV fracture and hydraulic fracture parameters (permeability, porosity, water saturation and compaction table).

4.6 Case II - History Matching

Based on sensitivity study as shown in previous section, the following sensitivity parameters have been chosen to do a history matching on field data:

1. Fracture porosity
2. SRV Fracture permeability – X,Z direction
3. Hydraulic fracture permeability– X,Z direction
4. SRV hydraulic fracture water saturation
5. Fracture compaction table
6. Hydraulic fracture compaction table
7. SRV and fracture dimension

Using the shortlisted set of parameters in the beginning of this section, we have used GA based software for history matching cumulative gas history data. History match comparison plots can be seen in **Figure 24(a), (b) and (c)** respectively.

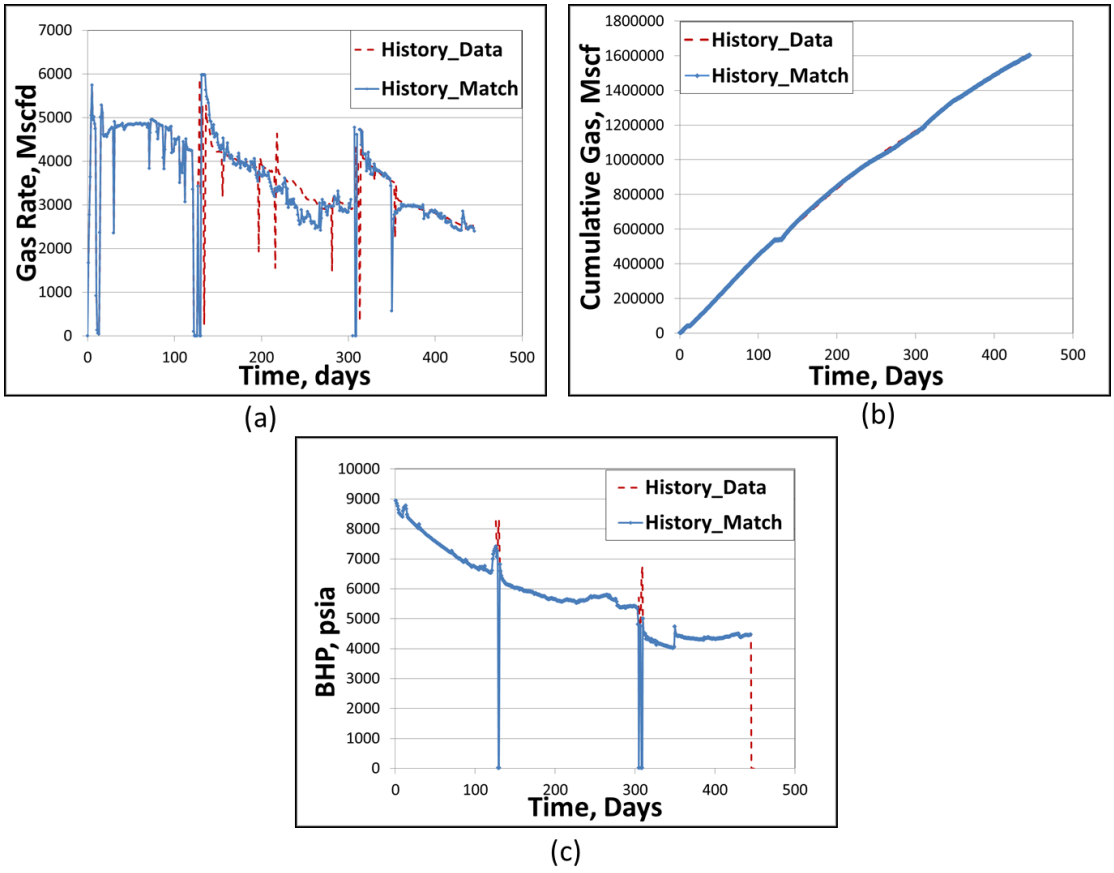

Figure 24: Comparison plot history data vs. history matched model (a) Gas production rate (b) Cumulative gas production (c) Bottom hole pressure

The goal of including SRV and hydraulic fracture dimension in sensitivity studies was to find an optimal dimension for parameters and to improve the match by reducing the misfit on cumulative gas rate. The above plots show a reasonable match for cumulative gas rate and we can see an improvement in gas rate match especially for last fifty days of production data.

CHAPTER V

FAST MARCHING METHOD – FIELD APPLICATION ON ANADARKO CASE STUDY*

This chapter includes Anadarko case study showing applications of fast marching method on a field case. At the time of this study, the extension of fast marching method had only been done for a dual porosity system. Hence, for the purpose of this application, the dual permeability model described in Chapter IV has been converted to a dual porosity model keeping rest of parameter distributions same. We have used a finite difference simulator for history matching purposes whereas fast marching method has been used for prediction study.

5.1 Case III - Model Description

This part of the study is based on a similar model as described in Case I. Following is the model property summary:

1. Dual porosity
2. Rock compaction and rock compressibility

*Certain sections reprinted with permission from "From Streamlines to Fast Marching: Rapid Simulation and Performance Assessment of Shale Gas Reservoirs Using Diffusive Time of Flight as a Spatial Coordinate" by Zhang, Y., Bansal, N., Fujita, Y., Datta-Gupta, A., King, M.J., Sankaran, S., 2014. Paper SPE 168997 presented at SPE Unconventional Resources Conference – USA, The Woodlands, Texas, USA, 1-3 April. Copyright 2014 by SPE.

3. Local grid refinement
4. SRV definition

It may be noted that property distributions for porosity, permeability and water saturation is same as Case I. The main difference between Case III and I is that in Case III we are using is a dual porosity model instead of a dual permeability model to represent the reservoir.

5.2 Case III - Sensitivity Study

Following the approach of Yin et al. (2011), to evaluate the impact of various parameters on production history, a set of selected parameters like permeability, porosity, water saturation and rock compaction factor have been chosen. **Table 9** shows a detailed list of selected parameters and the selected ranges for sensitivity studies. This study uses the SRV definition of the base case model.

Table 9: Parameter uncertainties for sensitivity and history matching – Case III

Uncertainty	Base	Low	High
SRV porosity (Frac_poro), fraction	1.00E-02	1.00E-03	5.00E-02
SRV fracture permeability in x direction (kx_frac), md	3.16E-02	3.16E-04	4.11E-02
SRV matrix permeability multiplier in x direction (kx_matrix)	1	1E-02	1.3
SRV fracture permeability in z direction (kz_frac) , md	3.16E-02	3.16E-04	4.11E-02
SRV matrix permeability multiplier in z direction (kz_matrix)	1	1E-02	1.3
Hydraulic fracture permeability-x direction (kx_hyd_frac),md	6.50E-01	6.50E-03	8.45E-01
Hydraulic fracture permeability-z direction (kz_hyd_frac),md	6.50E-01	6.50E-03	8.45E-01
SRV fracture water saturation (Sw_frac), fraction	2.00E-01	2.00E-03	2.40E-01
SRV hydraulic fracture water saturation (Sw_hyd_frac), fraction	7.00E-01	7.00E-03	8.40E-01
Fracture compaction table multiplier (Frac_comp)	1	0.6	1.5
Hydraulic fracture compaction table multiplier (Hyd_frac_comp)	1	0.6	1.5

Figure 25 shows a tornado diagram of the objective function (logarithm of cumulative gas misfit) with respect to selected parameters. All these parameters have been perturbed as per the ranges in **Table 9.**

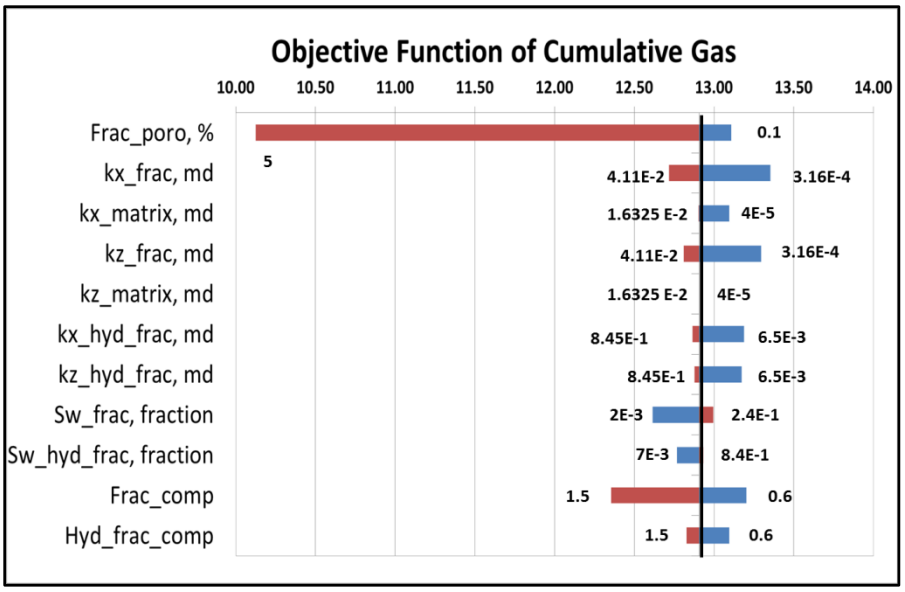

Figure 25: Tornado diagram of the objective function – logarithm of cumulative gas misfit

SRV fracture permeability along with compaction factors for fracture and hydraulic fractures have major impacts on cumulative gas misfit. Since it's a dual porosity model, matrix permeability has negligible sensitivity on objective function.

5.3 Case III - History Matching

Based on sensitivity study as shown in previous section, the following sensitivity parameters have been chosen to do a history matching on field data:

1. Fracture porosity
2. SRV Fracture permeability – X,Z direction
3. Hydraulic fracture permeability– X,Z direction
4. SRV fracture water saturation
5. Fracture compaction table

6. Hydraulic fracture compaction table

Comparison between history data and base case data (built based on model description section) is shown in Figure 26 (a), (b) and (c) respectively.

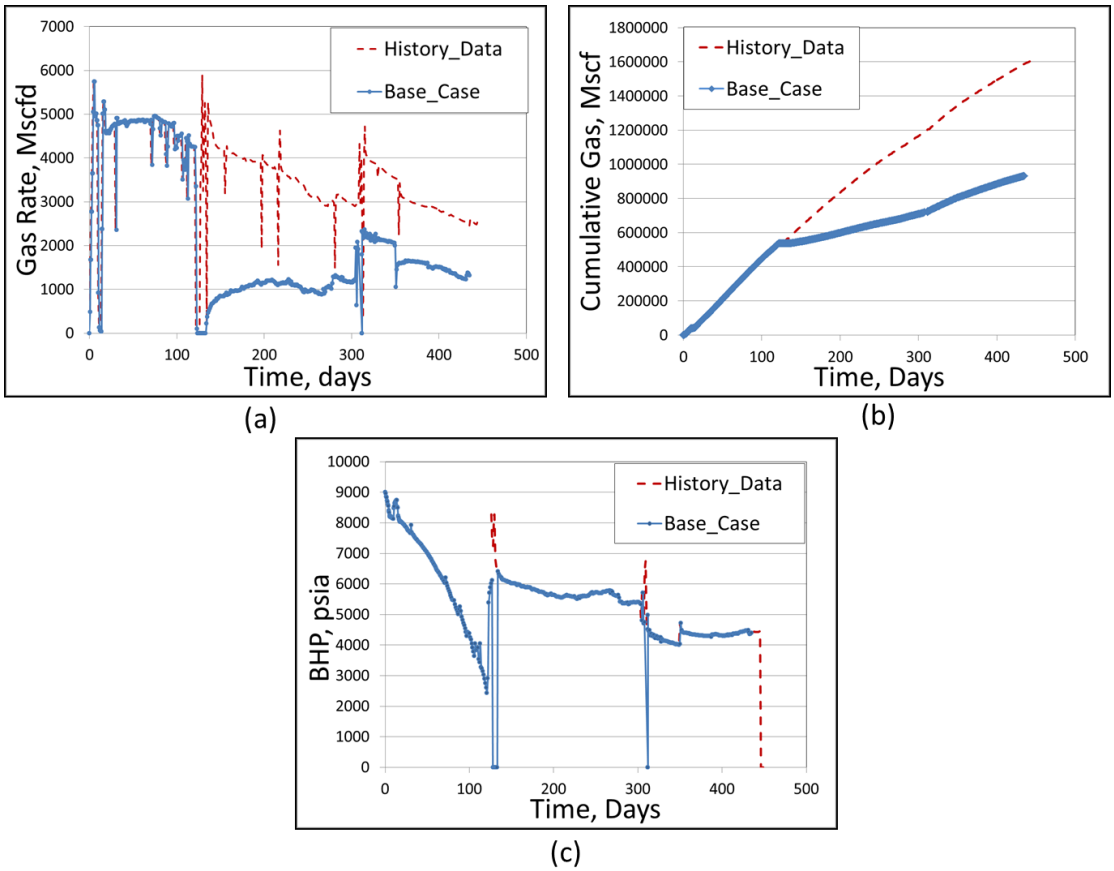

Figure 26: Comparison plot history data vs. base model output (a) Gas production rate (b) Cumulative gas production (c) Bottom hole pressure

Using the shortlisted set of parameters in the beginning of this section, we have used the GA based software for history matching cumulative gas rate data. For history matching

with GLOBAL, we have used a commercial finite difference simulator as a forward modeling tool. History match comparison results are shown in **Figure 27 (a), (b) and (c)** respectively.

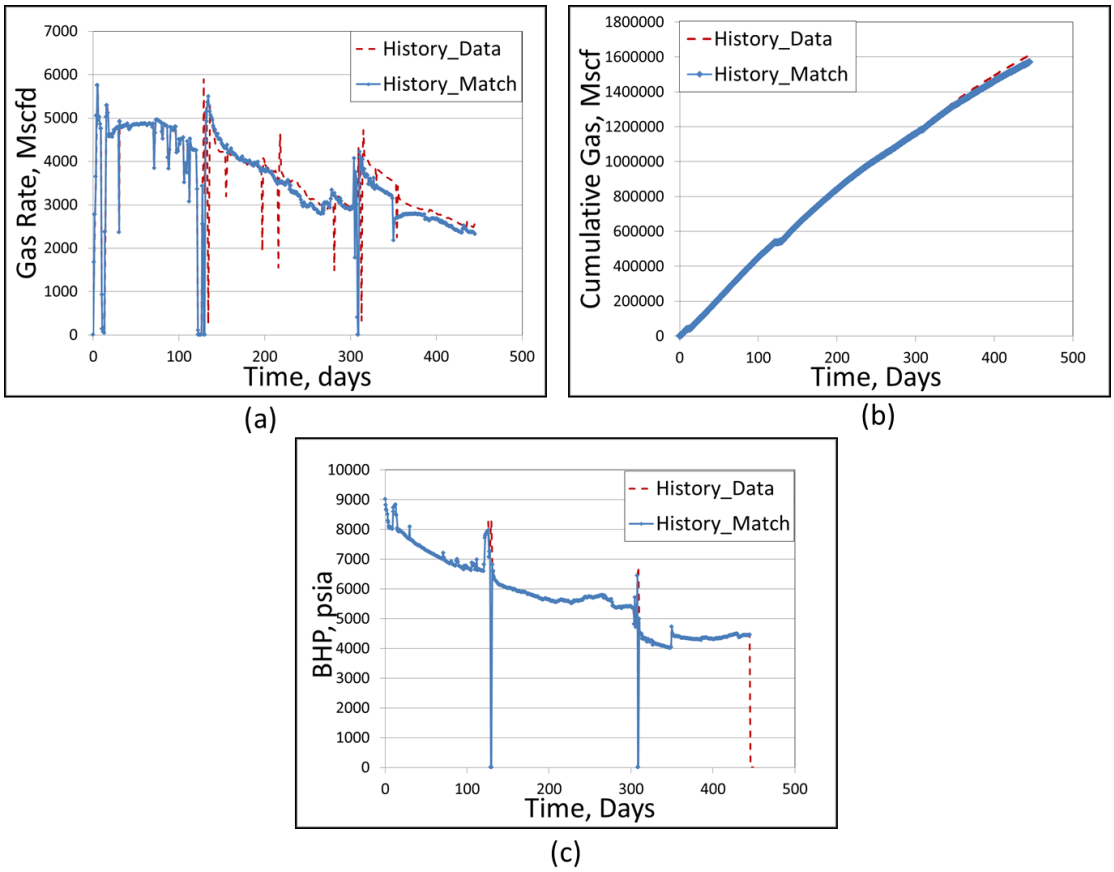

Figure 27: Comparison plot history data vs. history matched model (a) Gas production rate (b) Cumulative gas production (c) Bottom hole pressure

The comparison plot for the dual porosity model is a reasonable match for history data. The main reason of using this system is able to apply fast marching method for pressure

and rate solutions. Dual permeability solution using fast marching method is still under study.

Figure 28 (a) and (b) show the effect of history matching cumulative production data in the case study for reducing the parameter uncertainties. All the parameter ranges have been normalized to keep range between zero and unity. Only the parameters which show significant reduction in uncertainty are shown in the box plots. The range of every parameter is contained in the green and red box. After history match we can see tightening in parameter population range. In comparison to a dual permeability model this model is able to more effectively constraint the fracture permeability values as contribution as a conduit for production is not there from matrix. Matrix acts as the storage of hydrocarbons in a dual porosity model.

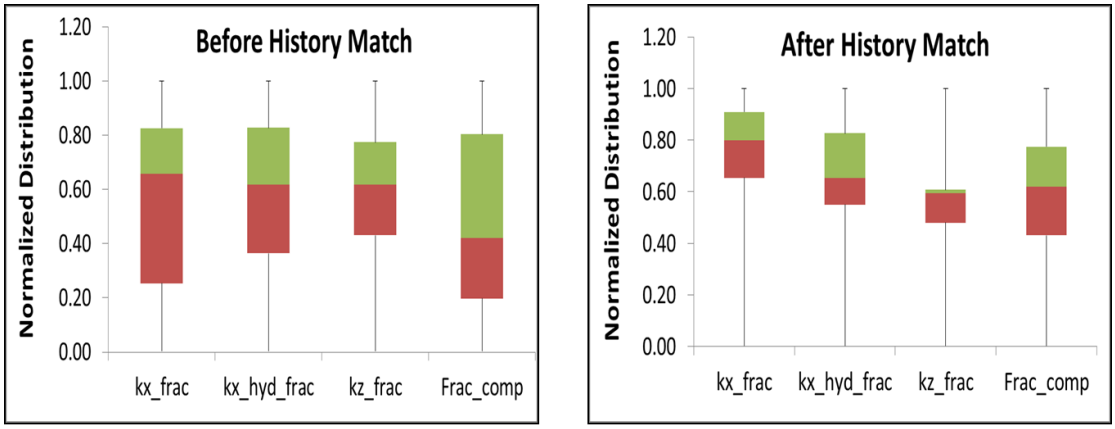

Figure 28: Uncertainty analysis of model by genetic algorithm – before history match

Although individual parameters cannot be constrained during history matching because of inherent non-uniqueness in inverse modeling, we have compared the total fracture half-length for all twenty two stags and plot the cumulative distribution function (CDF) for base and matched model as shown in Figure 29. We have examined the square root of fracture permeability times the summation of fracture half lengths. After history match a considerable tightening in range for composite parameter is observed.

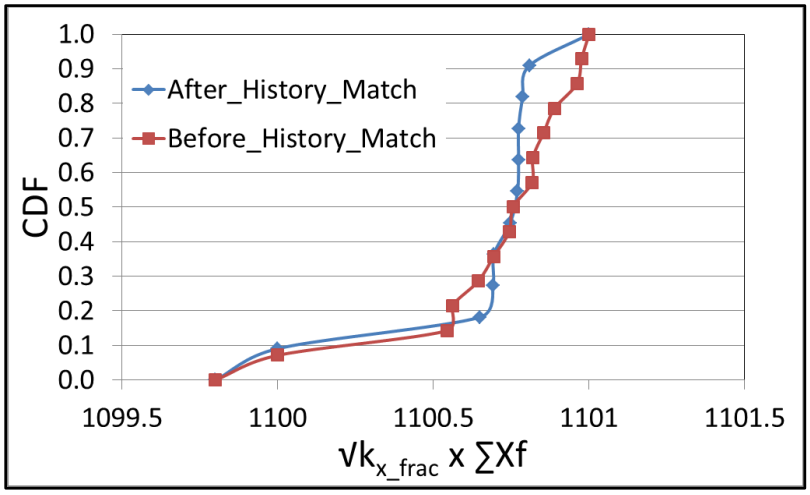

Figure 29: Distribution of square root of fracture permeability time fracture half-length summation- before and after history match

5.4 Case III - Fast Marching Method Comparison

This section shows the comparison study of fast marching method with FDSIM results for Case III history matched model. **Figure 30** shows the workflow used to FMM comparison study.

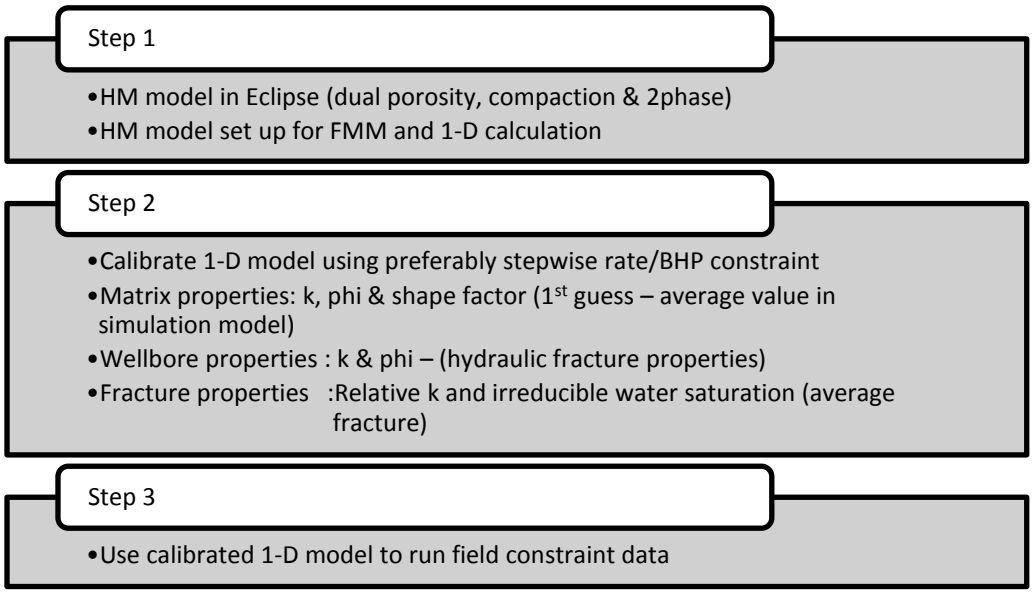

Figure 30: Workflow for pressure/rate solution for field study using 1-D solution

5.4.1 Step 1

For this step, Case III history matched model is used, which is a two phase, dual porosity system including compaction effects. To calculate diffusive time of flight we need only the fracture section of the dual porosity model as per explanation in CHAPTER II. After setting up the base case model with fractures alone, diffusive time of flight is calculated. 1D solution is then applied on to get pressure/rate outputs.

5.4.2 Step 2 & 3

1-D solution for the representative model in fast marching method includes constant values for matrix and wellbore properties. Arithmetic averages in model are chosen as base values for matrix properties (porosity, permeability and shape factor), wellbore

properties (porosity and permeability) and fracture properties – relative permeability and irreducible water saturation.

To decide on the representative values of these parameters, 1-D solution is run on the history matched model with a stepwise bottom hole pressure constraint (in this case). Matrix properties and fracture properties are manually modified around the average values to match the results from FDSIM simulation results. **Figure 31(a), (b) and (c)** show the results of history matched model with a stepwise bottom hole pressure constraint.

It may be noted that the calibration section of model was required for this study since FMM is still under evaluation to test generalize applicability to field cases. Fast marching method as a tool is expected to have direct applications for history matching in future. Considering the scope of this study, we have focused on comparing this tool with commercially available techniques in the industry.

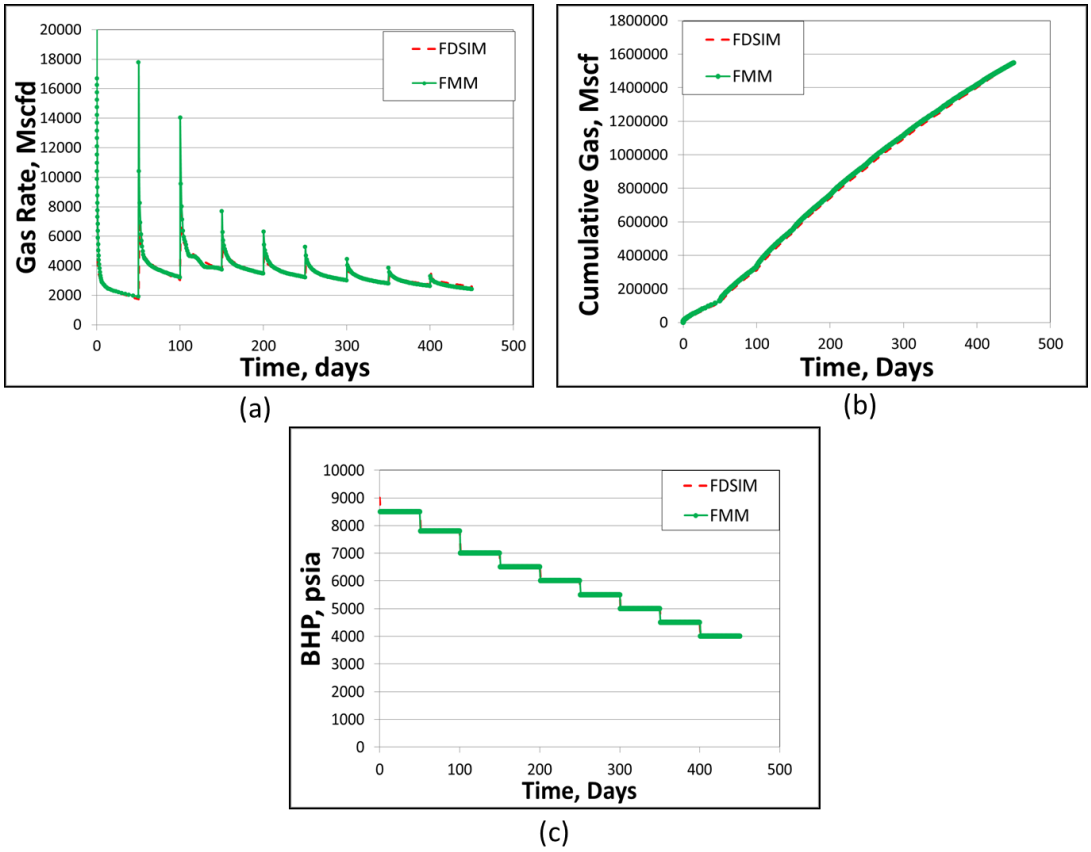

Figure 31: Comparison plot – well bottom hole pressure constraint; FDSIM vs. fast marching method (FMM) (a) Gas production rate (b) Cumulative gas production (c) Bottom hole pressure

Using the matched value of parameters, the history matched model is run with actual field history data. For the purpose of this run, we have used gas rate as a constraint for first 126 days of production and bottom hole pressure for remaining number of days. **Figure 32(a), (b) and (c)** show the comparison plots for history input data, FMM and FDSIM results respectively.

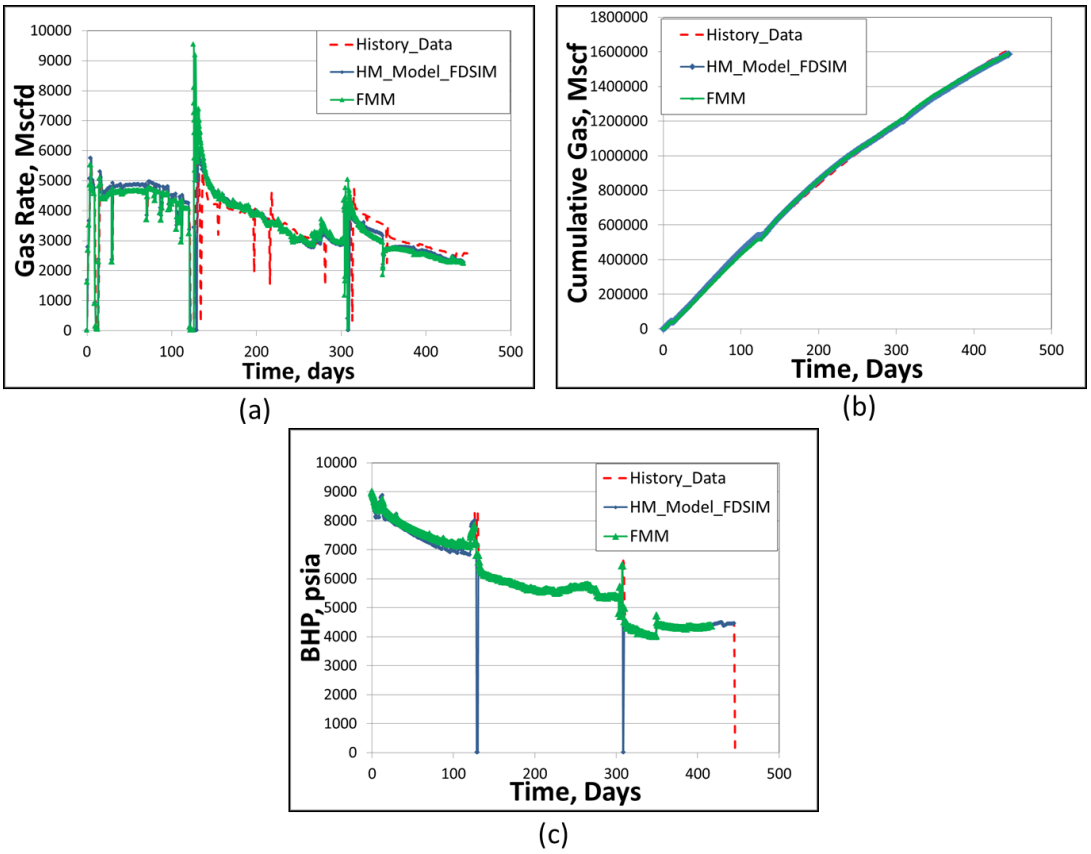

Figure 32: Comparison plot – well bottom hole pressure constraint; FDSIM vs. fast marching method (FMM) vs. history data (a) Gas production rate (b) Cumulative gas production (c) Bottom hole pressure

For the history matched model run with field history data, the fast marching results are well in agreement with FDSIM results.

5.5 Case IV - Model Description

This part of the study is mostly based on parameter and model definitions as per the given data set. The base model here is similar to Case II except this being a dual porosity model. Other than the reservoir parameters like porosity, permeability, water saturation,

compaction table; SRV width, Fracture height, Fracture width are the additional sensitivity parameters as done in Case II.

5.6 Case IV - Sensitivity Study

Table 10 shows a detailed list of selected parameters and the selected ranges for sensitivity study. **Figure 33(a) and (b)** show tornado diagrams of the objective function (logarithm of cumulative gas misfit) with respect to selected parameters as per **Table 10**.

Table 10: Parameter uncertainties for sensitivity and history matching – Case IV

Uncertainty Parameter (variables defined)	Base	Low	High
SRV fracture porosity (Frac_poro1, Frac_poro2, Frac_poro3, Frac_poro4)	0.01	0.001	0.05
SRV fracture permeability in x direction, md (kx_frac1, kx_frac2 , kx_frac3, kx_frac4)	0.0316	0.000316	0.0411
SRV hydraulic fracture permeability in x direction, md (kx_hyd_frac1, kx_hyd_frac2, kx_hyd_frac3, kx_hyd_frac4)	0.650	0.0065	6.5
SRV matrix permeability multiplier in x direction, md ((kx_matrix1, kx_ matrix2, kx_ matrix3, kx_ matrix4)	1	0.01	1.3
SRV hydraulic fracture permeability in z direction, md (kz_hyd_frac1, kz_hyd_frac2, kz_hyd_frac3, kz_hyd_frac4)	0.0316	0.000316	0.0411
SRV hydraulic fracture permeability in z direction, md (kz_hyd_frac1, kz_hyd_frac2, kz_hyd_frac3, kz_hyd_frac4)	0.65	0.0065	6.5
SRV matrix permeability multiplier in z direction, md ((kz_matrix1, kz_ matrix2, kz_ matrix3, kz_ matrix4)	1	0.01	1.3
SRV fracture water saturation (Sw_frac1, Sw_frac2, Sw_frac3, Sw_frac4)	0.2	0.002	0.24
SRV hydraulic fracture water saturation (Sw_hyd_frac1, Sw_hyd_frac2, Sw_hyd_frac3, Sw_hyd_frac4)	0.7	0.007	0.84
Fracture compaction table multiplier (Frac_comp)	1	0.6	1.5
Hydraulic fracture compaction table multiplier (Hyd_frac_comp)	1	0.6	1.5
Fracture half length, ft (Frac_W1, Frac_W2, Frac_W3, Frac_W4)	150	50	250
Fracture height, ft (Frac_H1, Frac_H2, Frac_H3, Frac_H4)	60	30	90
SRV width, ft (SRV_W1, SRV_W2, SRV_W3, SRV_W4)	350	250	650

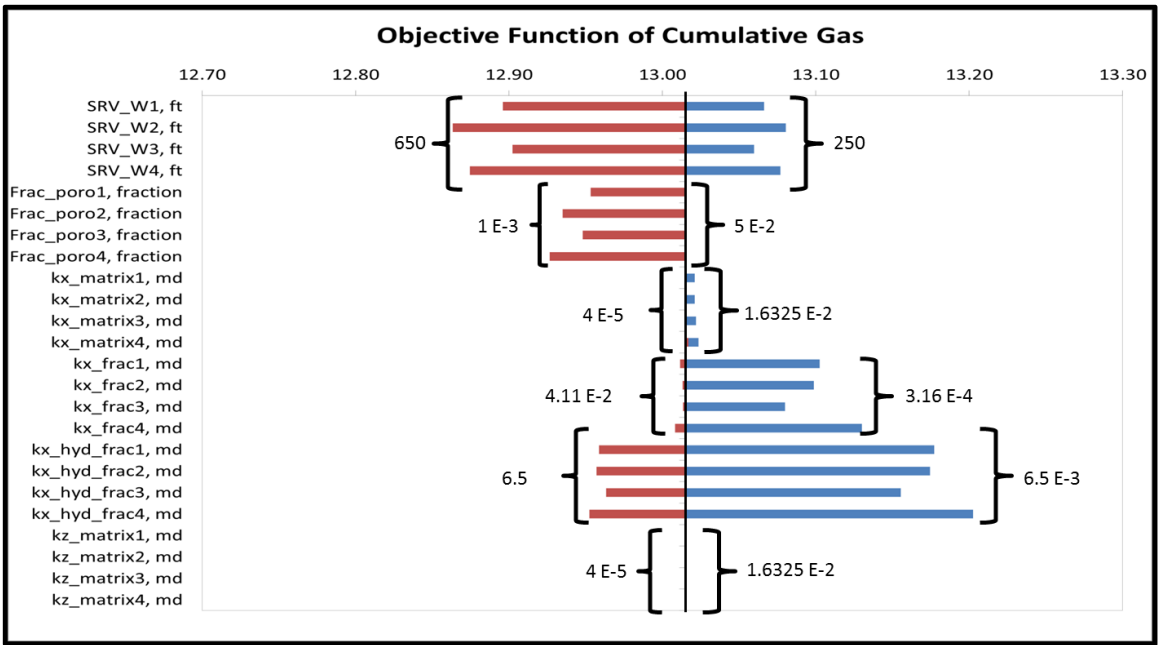

(a)

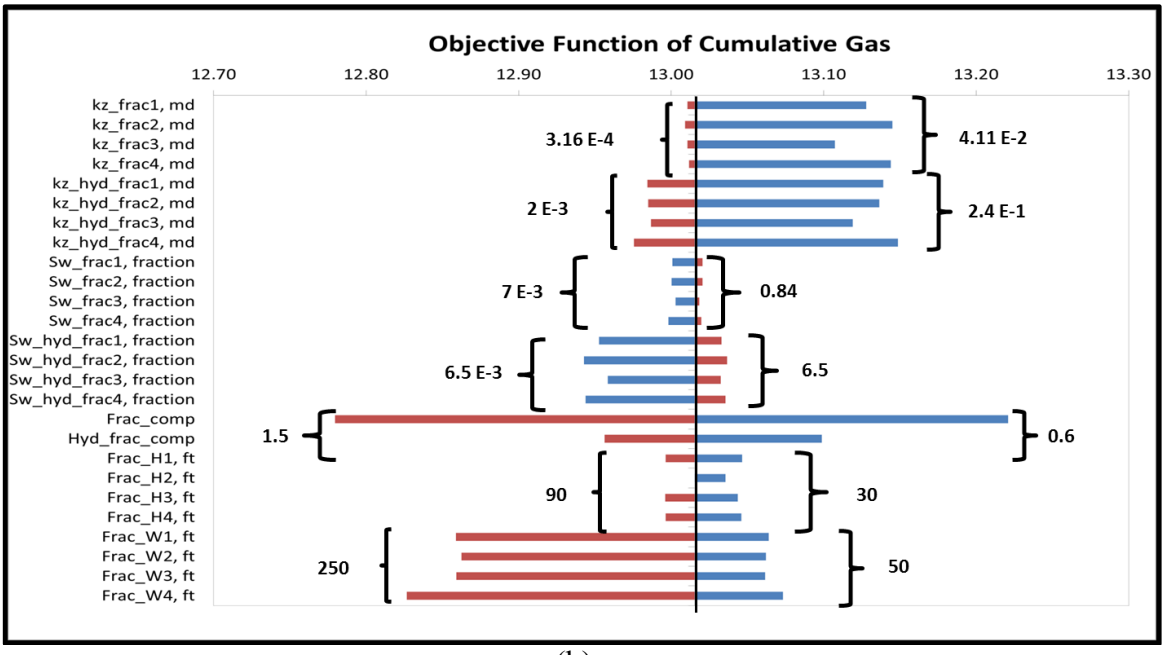

(b)

Figure 33(a), (b): Tornado diagrams of the objective function – logarithm of cumulative gas misfit

From the tornado diagrams it can be seen that SRV and fracture size has a major impact on cumulative gas misfit along with SRV fracture and hydraulic fracture parameters (permeability, porosity and water saturation). Since this is a dual porosity case, not much sensitivity can be seen for matrix permeability.

5.7 Case IV - History Matching & FMM Comparison

Based on sensitivity study as shown in previous section, the following sensitivity parameters have been chosen to do a history matching on field data:

1. Fracture porosity
2. SRV Fracture permeability – X,Z direction
3. Hydraulic fracture permeability– X,Z direction
4. SRV fracture water saturation
5. Fracture compaction table
6. Hydraulic fracture compaction table
7. SRV and Fracture width

History match results can be seen in **Figure 34 (a), (b) and (c)** respectively. The history match in Case IV has visibly improved compared to Case III. **Figure 35 (a) and (b)** show the effect of history matching cumulative production data in reducing the parameter. The plots only show the normalized distribution of parameters having maximum reduction in uncertainty. The range of every parameter is contained in the green and red box. After history match we can see tightening in parameter population

range. **Figure 36** illustrates the fracture dimension change for before and after history match for one of the history matched cases.

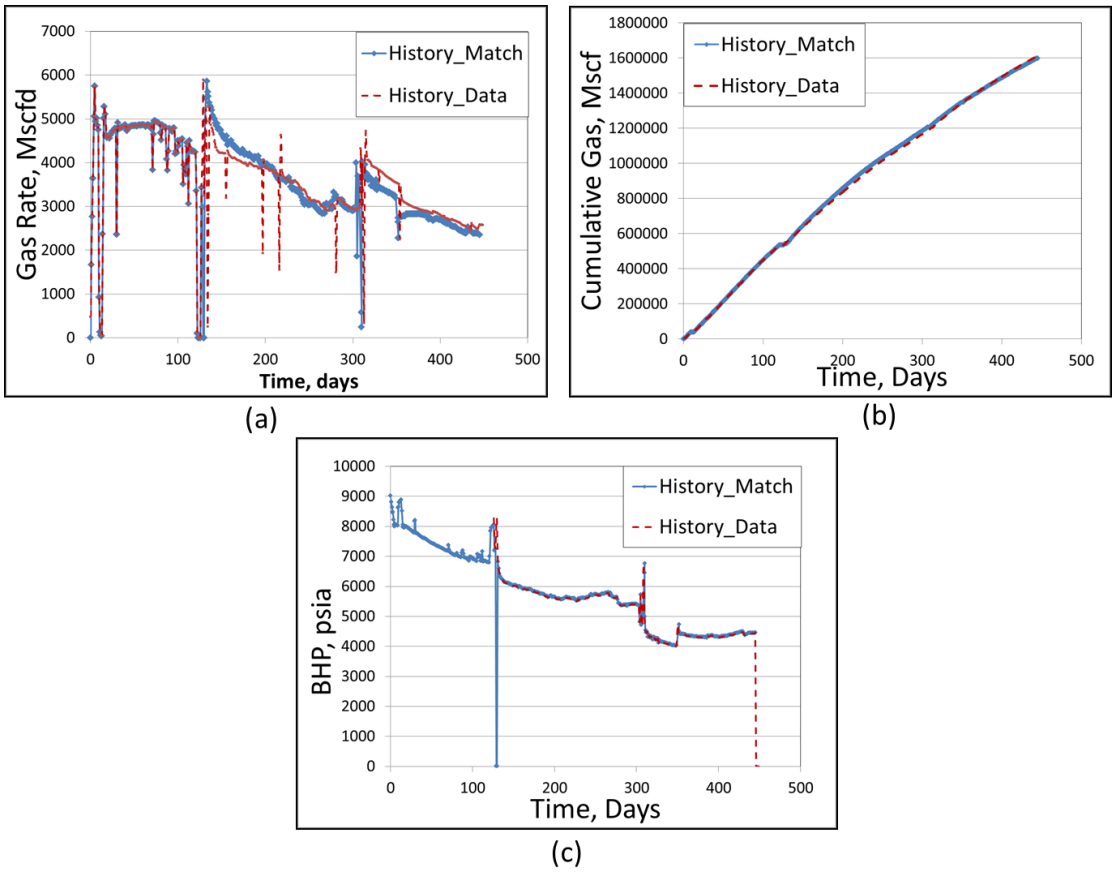

Figure 34: Comparison plot history data vs. history matched model (a) Gas production rate (b) Cumulative gas production (c) Bottom hole pressure

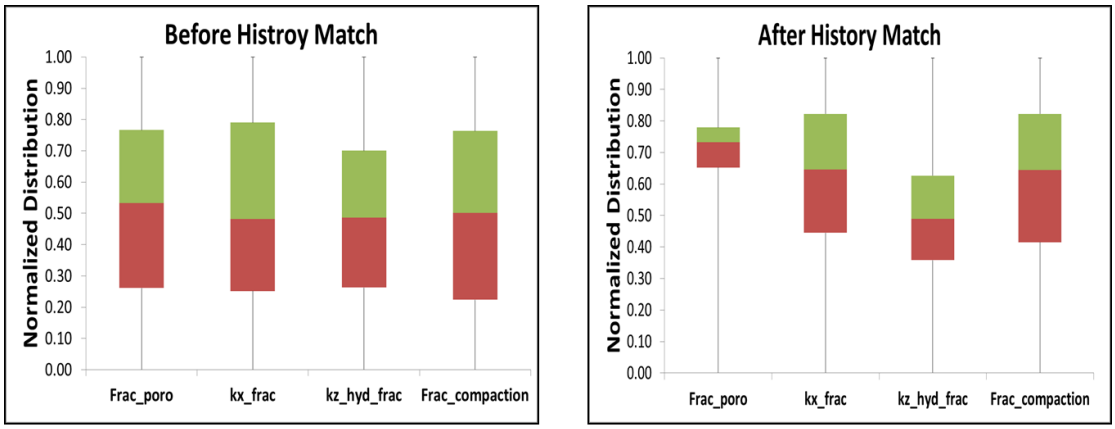

(a) (b)

Figure 35: Uncertainty analysis of model by genetic algorithm (a) Before history match (b) After history match

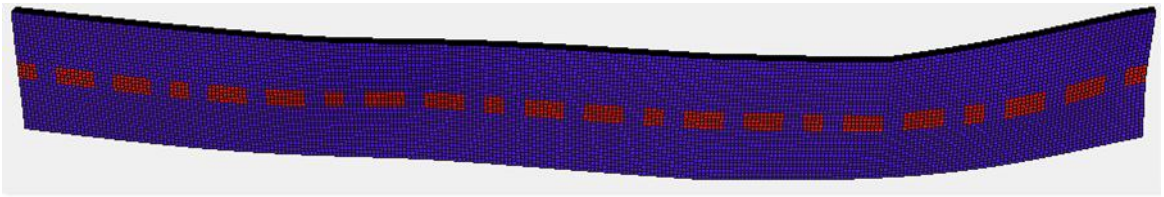

(a)

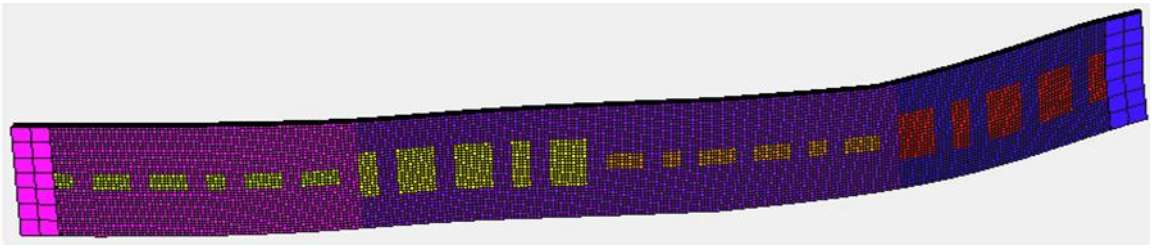

(b)

Figure 36: Comparison of fracture dimensions (a) Before history match (b) After history match

Now we applied the same workflow as explained in the beginning of section 5.4 for comparing results from fast marching method and commercial simulator.

Figure 37(a), (b) and (c) show the comparison plots for history input data, FMM and FDSIM results.

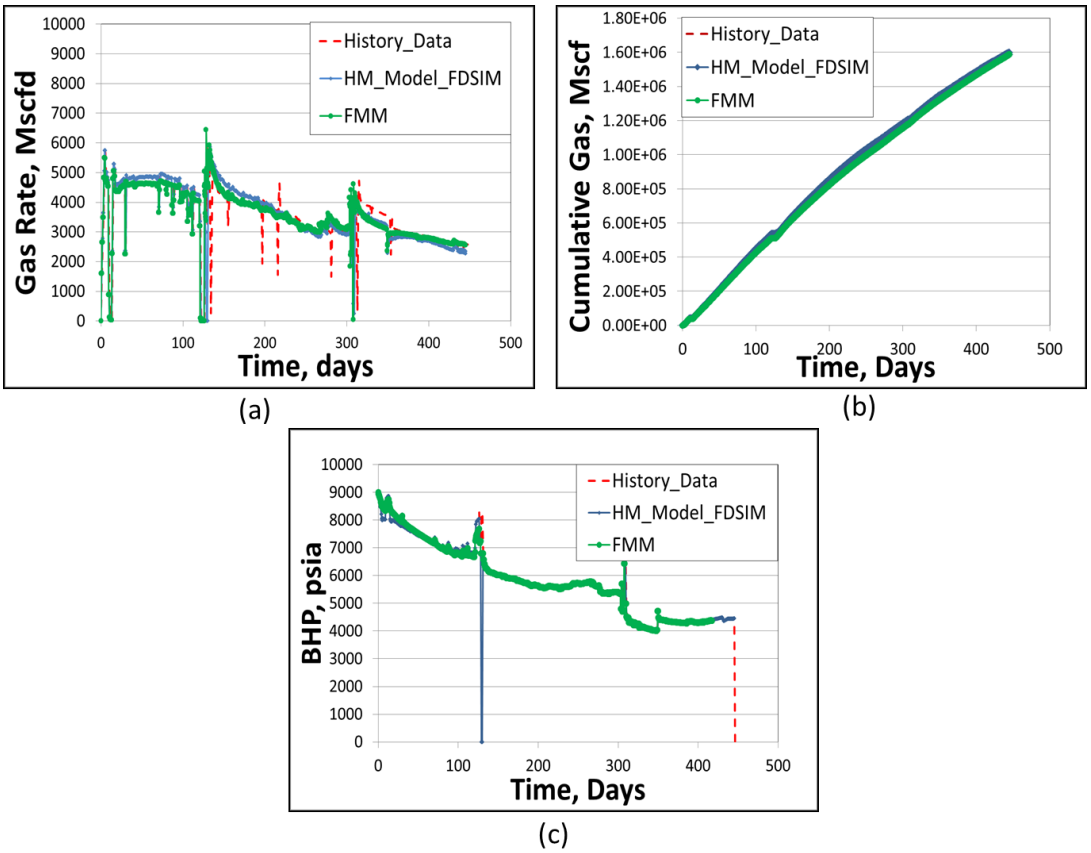

Figure 37: Comparison plot history data vs. history matched model vs. FMM (a) Well gas rate (b) Well cumulative gas rate (c) Well bottom hole pressure

The comparison plots for fast marching method matches well with history data and commercial simulator. The main advantage for fast marching method comes with the computation speed along with the capability to handle reservoir information effectively.

Although, there is scope of improvement in algorithm we have currently used. Also, as we are able to test the method with more field cases, we would have more clarity on its capabilities.

5.8 Prediction Study

We had additional 400 days of production data for prediction studies. For this study we have used bottom hole pressure as the production constraint after ~127 days to predict cumulative gas rate production from the well in consideration. The plots shown in this section will have ~450 days of history matched data along with 400 days of prediction study data. Prediction comparison plots for Case IV history matched model are shown in **Figure 38(a), (b) and (c)** respectively.

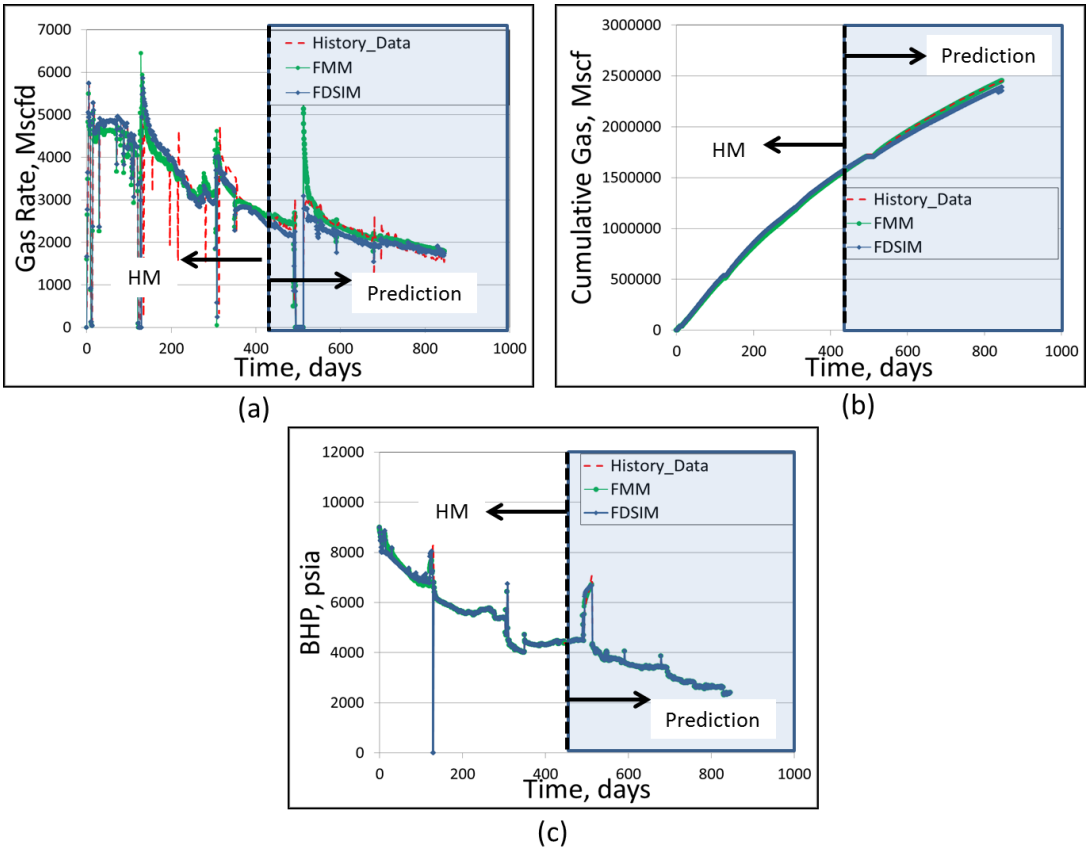

Figure 38: Reservoir performance prediction after the history matching (a) Gas Production rate (b) Cumulative gas production (c) Bottom hole pressure

The comparison plots include history data and predictions using fast marching method and finite difference simulator (FDSIM). The comparison study shows that FMM is able to reasonably predict the field history using the matched model.

CHAPTER VI

SUMMARY AND CONCLUSIONS*

The main objective of this work has been to present and summarize the techniques available for characterizing unconventional reservoirs, including decline curve analysis, diagnostic methods but primarily focusing on fast matching method. FMM has proven its ability with respect to speed in a number of studies conducted by previous authors as well as in this case. This work presents the first field study done using fast marching method. The method has been tested on a dual porosity model and has shown comparable results with the available techniques.

Due to limitations on seismic data, the case models in this study are limited to a layer cake system with limited areal heterogeneity. The case study in consideration is a tight formation and hence, the drainage mainly happens in the SRV region. Keeping this in mind the property distribution in SRV region has been the focus in our sensitivity studies. Case I and Case III use uniform SRV properties for history matching whereas in Case II and Case IV we introduce heterogeneity in SRV by grouping four regions.

---

*Certain sections reprinted with permission from "From Streamlines to Fast Marching: Rapid Simulation and Performance Assessment of Shale Gas Reservoirs Using Diffusive Time of Flight as a Spatial Coordinate" by Zhang, Y., Bansal, N., Fujita, Y., Datta-Gupta, A., King, M.J., Sankaran, S., 2014. Paper SPE 168997 presented at SPE Unconventional Resources Conference – USA, The Woodlands, Texas, USA, 1-3 April. Copyright 2014 by SPE.

Rate transient analysis on the production data gives complementary results to the simulation study. Analytical study was mainly helpful to give an estimate for SRV definition. Given the missing pressure data in early part of production history, fracture related details could not be captured effectively in this case.

Genetic algorithm based software has been used for sensitivity study and history matching the field case study using a FD simulator. All the field case study models have been matched on cumulative gas rate. During sensitivity study, fracture properties such as permeability, porosity, water saturation and compaction have been the common heavy hitters. Matrix properties show nearly negligible impact on sensitivity for dual porosity models.

Sensitivity study in all cases has been followed by history matching. For the cases presented, the history matched model is able to give reasonable match for the field history data. On comparison, dual porosity models show slightly more parameter uncertainty reduction for some parameters in comparison to dual permeability models. Further, for cases with SRV region grouping the matched models show lesser tightening in parameter range distribution in comparison to uniform property case. The uncertainty reduction in such cases gets distributed amongst four parameters instead of one.

For the purpose of this study, fast marching method model has been calibrated against a commercial FDSIM. The calibrated FMM model has been used for prediction studies. Following are some of the key concepts learned from this work:

1. We have analyzed production data from a shale gas reservoir using rate transient analysis.
2. A 3-D reservoir model was set up based on the parameters from the rate transient analysis.
    a. Dual permeability model (DPDP)
    b. Dual porosity model (DPSP)
3. Sensitivity studies were carried to identify the 'heavy hitters'
4. Assisted history matching using Genetic algorithm using FDSIM was successful in reproducing the field production history
    a. The history matching was able to constrain fracture permeability, porosity and in some cases matrix porosity as well as rock compaction
5. This work has demonstrated the feasibility of using the FMM as a forward model during assisted history matching of unconventional reservoirs
6. The FMM results are shown to be consistent with finite difference simulation – but with a much faster computation time.

This work tested a novel method to perform rapid simulation and performance assessment of shale gas reservoirs. This method is based on a coordinate transformation from the physical space to the one-dimensional DTOF space derived from the FMM

solution. The approach is analogous to the streamline method which is widely used in the industry for modeling convective flow in the reservoir. As in streamline methods, the DTOF coordinate (τ-coordinate) embeds the reservoir heterogeneity and reduces the heterogeneous 3-D problem into a 1-D homogeneous problem in the τ-coordinate without explicit trajectory tracing. This allows the 3-D diffusivity equation to be written into a 1-D equation in τ-coordinate, which can be solved using FD, in a manner analogous to the calculation along a single streamline.

Application of the new method is well suited for rapid simulation and performance assessment of Shale Gas reservoirs under very general conditions of reservoir heterogeneity and changing well production schedules. We have benchmarked the results of the new method against a commercial reservoir simulator for validation purposes using a synthetic example and a field example. For the example cases studied, the proposed method is able to produce comparable results with up to an order of magnitude increase in the simulation speed. In the field case study of a shale gas reservoir in east Texas, we have applied the new method together with the genetic algorithm to successfully identify key reservoir uncertainties, perform history matching, and make reservoir performance predictions.

6.1 Recommendations for Future Work

Although results from fast marching method on our first field study are encouraging, there is scope of improvement in method and future work. Following are some of the areas identified for future work:

1. Fast marching method needs to be linked to Global - GA based software.
2. Current algorithm for 1-D solution can be improved to handle field production data more efficiently, which can bring down the run time for fast marching method further.
3. Extension of time of flight algorithm to handle local grid refinement
4. Extending algorithm to handle compositional and multiphase models will be helpful to test and eventually apply on field case studies.
5. 1-D solution can be modified to handle a dual permeability model to further increase field applications.

REFERENCES

Araya, A. and Ozkan, E. 2002. An Account of Decline-Type-Curve Analysis of Vertical, Fractured, and Horizontal Well Production Data. Paper presented at the SPE Annual Technical Conference and Exhibition, San Antonio, Texas. Copyright 2002, Society of Petroleum Engineers Inc. 00077690. DOI: 10.2118/77690-ms.

Arps, J.J. 1945. Analysis of Decline Curves. *Trans*. AIME, **160**: 228-247. Society of Petroleum Engineers SPE-945228-G. DOI: 10.2118/945228-g.

Can, B. and Kabir, C.S. 2011. Probabilistic Performance Forecasting for Unconventional Reservoirs with Stretched-Exponential Model. Paper presented at the North American Unconventional Gas Conference and Exhibition, The Woodlands, Texas. Society of Petroleum Engineers SPE-143666-MS. DOI: 10.2118/143666-ms.

Carter, R.D. 1985. Type Curves for Finite Radial and Linear Gas-Flow Systems: Constant-Terminal-Pressure Case. *Society of Petroleum Engineers Journal,* **25** (5): 719-728. DOI: 10.2118/12917-pa.

Crafton, J.W. Oil and Gas Well Evaluation Using the Reciprocal Productivity Index Method. Paper presented at the SPE Production Operations Symposium, Oklahoma City, Oklahoma. Copyright 1997, Society of Petroleum Engineers, Inc. 00037409. DOI: 10.2118/37409-ms.

Datta-Gupta, A., Xie, J., Gupta, N., King, M. J. and Lee W. J. 2011, Radius of Investigation and its Generalization to Unconventional Reservoirs, *Journal of Petroleum Technology*, **63** (7): 52-55.

Fetkovich, M.J. 1980. Decline Curve Analysis Using Type Curves. *Journal of Petroleum Technology,* **32** (6): 1065-1077. DOI: 10.2118/4629-pa.

Ilk, D., Anderson, D.M., Stotts, G.W.J. et al. 2010. Production Data Analysis--Challenges, Pitfalls, Diagnostics. *SPE Reservoir Evaluation & Engineering,* **13** (3): pp. 538-552. DOI: 10.2118/102048-pa.

Ilk, D., Broussard, N.J., and Blasingame, T.A. 2012. Production Analysis in the Eagle Ford Shale -- Best Practices for Diagnostic Interpretations, Analysis, and Modeling. Paper presented at the SPE Annual Technical Conference and Exhibition, San Antonio, Texas. Society of Petroleum Engineers SPE-160076-MS. DOI: 10.2118/160076-ms.

Ilk, D., Rushing, J.A., Perego, A.D. et al. 2008. Exponential Vs. Hyperbolic Decline in Tight Gas Sands — Understanding the Origin and Implications for Reserve Estimates Using Arps' Decline Curves. Paper presented at the SPE Annual Technical Conference and Exhibition, Denver, Colorado. Society of Petroleum Engineers SPE-116731-MS. DOI: 10.2118/116731-ms.

Kabir, S., Rasdi, F., and Igboalisi, B. 2011. Analyzing Production Data from Tight Oil Wells. *Journal of Canadian Petroleum Technology,* **50** (5): pp. 48-58. DOI: 10.2118/137414-pa.

Lee, W.J. 1982. *Well Testing*. Society of Petoleum Engineers, Richardson, Texas.

Marhaendrajana, T. and Blasingame, T.A. 2001. Decline Curve Analysis Using Type Curves - Evaluation of Well Performance Behavior in a Multiwell Reservoir System. Paper presented at the SPE Annual Technical Conference and Exhibition, New Orleans, Louisiana. 2001. Society of Petroleum Engineers Inc. 00071517. DOI: 10.2118/71517-ms.

Mattar, L. 2008. Production Analysis and Forecasting of Shale Gas Reservoirs: Case History-Based Approach. Paper presented at the SPE Shale Gas Production Conference, Fort Worth, Texas. Society of Petroleum Engineers SPE-119897-MS. DOI: 10.2118/119897-ms.

Medeiros, F., Kurtoglu, B., Ozkan, E. et al. 2010. Analysis of Production Data from Hydraulically Fractured Horizontal Wells in Shale Reservoirs. *SPE Reservoir Evaluation & Engineering,* **13** (3): pp. 559-568. DOI: 10.2118/110848-pa.

Palacio, J.C. and Blasingame, T.A. 1993. Decline-Curve Analysis with Type Curves – Analysis of Gas Well Production Data. Paper presented at the Rocky Mountain Region/Low Permeability Reservoirs Symposium and Exhibition, Denver, 12-14 April. Society of Petroleum Engineers SPE-25909-MS. DOI: 10.2118/25909-ms.

Sethian, J. A. 1996. A Fast Marching Level Set Method for Monotonically Advancing Fronts. *Proceedings of the National Academy of Science,* **93**: 1591-1595.

Sethian, J. A. 1999. Fast Marching Methods.*SIAM Review,* **41**: 199-235.

Sethian, J. A. and Vladimirsky, A. 2000. Fast Methods for Eikonal and Related Hamilton-Jacobi Equations on Unstructured Meshes. *Proceedings of the National Academy of Science,* **97**: 5699-5703.

Slider, H.C. 1968. A Simplified Method of Hyperbolic Decline Curve Analysis. *Journal of Petroleum Technology:* 235-236. Society of Petroleum Engineers SPE-1936-PA. DOI: 10.2118/1936-pa.

Valko, P.P. 2009. Assigning Value to Stimulation in the Barnett Shale: A Simultaneous Analysis of 7000 Plus Production Histories and Well Completion Records. Paper presented at the SPE Hydraulic Fracturing Technology Conference, The Woodlands, Texas. Society of Petroleum Engineers SPE-119369-MS. DOI: 10.2118/119369-ms.

Valko, P.P. and Lee, W.J. 2010. A Better Way to Forecast Production from Unconventional Gas Wells. Paper presented at the SPE Annual Technical Conference and Exhibition, Florence, Italy. Society of Petroleum Engineers SPE-134231-MS. DOI: 10.2118/134231-ms.

Xie, J., Gupta, N., King, M.J. et al. 2012a. Depth of Investigation and Depletion Behavior in Unconventional Reservoirs Using Fast Marching Methods. Paper presented at the SPE Europec/EAGE Annual Conference, Copenhagen, Denmark. Society of Petroleum Engineers SPE-154532-MS. DOI: 10.2118/154532-ms.

Xie, J., Yang, C., Gupta, N. et al. 2012b. Integration of Shale Gas Production Data and Microseismic for Fracture and Reservoir Properties Using Fast Marching Method. Paper presented at the SPE Eastern Regional Meeting, Lexington, Kentucky. Society of Petroleum Engineers SPE-161357-MS. DOI: 10.2118/161357-ms.

Yin, J., Xie, J., Datta-gupta, A. et al. 2011. Improved Characterization and Performance Assessment of Shale Gas Wells by Integrating Stimulated Reservoir Volume and Production Data. Paper presented at the SPE Eastern Regional Meeting, Columbus, Ohio. Society of Petroleum Engineers SPE-148969-MS. DOI: 10.2118/148969-ms.

Zhang, Y., Yang, C., King, M. et al. 2013. Fast-Marching Methods for Complex Grids and Anisotropic Permeabilities: Application to Unconventional Reservoirs. Paper presented at the 2013 SPE Reservoir Simulation Symposium, The Woodlands, Texas. Society of Petroleum Engineers SPE-163637-MS. DOI: 10.2118/163637-ms.

Zhang, Y., Bansal, N., Fujita, Y., Datta-Gupta, A., King, M.J., Sankaran, S., 2014. From Streamlines to Fast Marching: Rapid Simulation and Performance Assessment of Shale Gas Reservoirs Using Diffusive Time of Flight as a Spatial Coordinate. Paper presented at SPE Unconventional Resources Conference – USA, The Woodlands, Texas. Society of Petroleum Engineers SPE-168997-MS.

APPENDIX

FAST MARCHING METHOD - OBSERVATIONS

A.1 Background

We have observed that for Case III i.e. dual porosity model with fixed SRV and hydraulic fracture dimensions has some differences in contours of diffusive time of flight and pressure contours generated using FDSIM. This section describes the probable reason for such a difference in contours generated using two techniques. **Figure A1** shows a cross-section view of pressure map (JK section) using finite difference simulator. Contour map shows there is some pressure drop in entire SRV region before any pressure drop outside SRV region. A certain preference has been seen to drain right side of model before left side. This effect can be attributed to perforation located at edge of SRV (well kick of point) on right hand side of model.

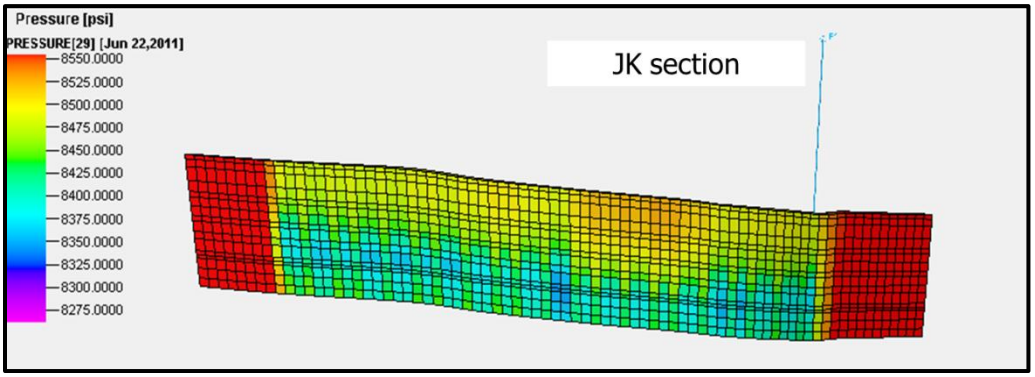

Figure A1: Pressure map: JK section Case III

Figure A2 shows a view of DTOF map (JK section) using fast marching method. We can clearly see that there is preference to drain right side of model before most of the SRV region itself. The reason being, time of flight calculation is directly proportional to porosity to permeability ratio. The porosity distribution in this case a constant value assigned to inside SRV region and a much lower value of porosity for outside SRV region. Hence local minimum for time of flight calculations for outside SRV region will be less than inside SRV; resulting in a preferential drainage happening outside SRV region.

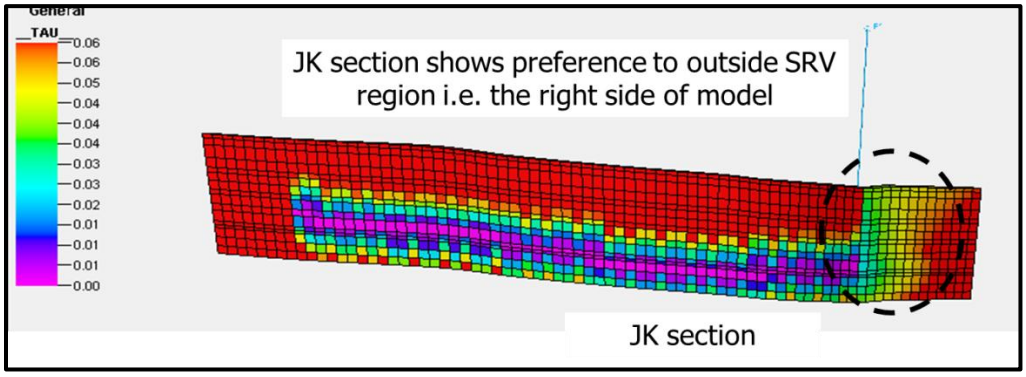

Figure A2: DTOF map: JK section Case III

Figure A3 shows a view of DTOF map (JK section) using fast marching method for Case IV .In this case we use variable SRV and hydraulic fracture dimensions and property distribution. As mentioned previously, this case has inside SRV region property distributed into four groups.

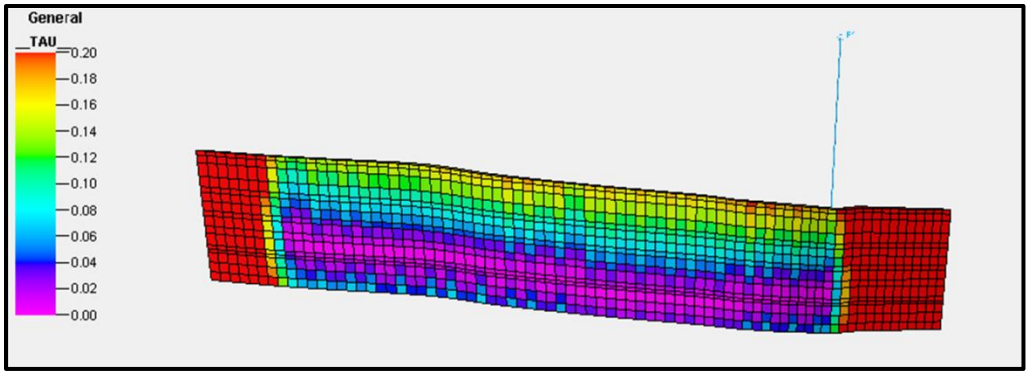

Figure A3: DTOF map: JK section Case IV

Case IV DTOF map shows preferential drainage to SRV region which seems more logical for a horizontal hydraulically fractured well. Our study shows that DTOF calculation is more sensitive to property distribution (porosity and permeability) than a finite difference simulator. Our approach is based on wave theory in comparison to the conventionally used mass balance approach in commercial simulators. In certain models like Case III, DTOF map can help bring out issues with physical viability of a model. At the same time, we need to be careful with property distribution in model while using fast marching method, given its sensitivity and background of the approach itself.